Science of the Total Environment 806 (2022) 150435

Contents lists available at ScienceDirect

Science of the Total Environment

journal homepage: www.elsevier.com/locate/scitotenv

# Contrasting land-uses in two small river basins impact the colored dissolved organic matter concentration and carbonate system along a river-coastal ocean continuum

Elizabeth D. Curra-Sánchez [a,b,c], Carlos Lara [d,e], Marcela Cornejo-D'Ottone [f], Jorge Nimptsch [g], Mauricio Aguayo [h], Bernardo R. Broitman [c,i], Gonzalo S. Saldías [c,j], Cristian A. Vargas [b,c,*]

[a] Programa de Doctorado en Ciencias Ambientales, Departamento de Sistemas Acuáticos, Facultad de Ciencias Ambientales, Universidad de Concepción, Concepción, Chile
[b] Laboratorio de Ecosistemas Costeros y Cambio Ambiental Global (ECCALab), Departamento de Sistemas Acuáticos, Facultad de Ciencias Ambientales y Centro de Ciencias Ambientales EULA Chile, Universidad de Concepción, Concepción, Chile
[c] Instituto Milenio en Socio-Ecología Costera (SECOS), P. Universidad Católica de Chile, Santiago, Chile
[d] Departamento de Ecología, Facultad de Ciencias, Universidad Católica de la Santísima Concepción, Concepción, Chile
[e] Centro de Investigación en Recursos Naturales y Sustentabilidad, Universidad Bernardo O'Higgins, Santiago, Chile
[f] Escuela de Ciencias del Mar, Pontificia Universidad Católica de Valparaíso, Valparaíso, Chile
[g] Instituto de Ciencias Marinas y Limnológicas, Laboratorio de Bioensayos y Limnología Aplicada, Facultad de Ciencias, Universidad Austral de Chile, Valdivia, Chile
[h] Departamento de Planificación Territorial, Facultad de Ciencias Ambientales y Centro de Ciencias Ambientales EULA Chile, Universidad de Concepción, Concepción, Chile
[i] Departamento de Ciencias, Facultad de Artes Liberales, Universidad Adolfo Ibáñez, Viña del Mar, Chile
[j] Departamento de Física, Facultad de Ciencias, Universidad del Bío-Bío, Concepción, Chile

## HIGHLIGHTS

- Contrasting land use in basins influences CDOM proportions in river-coastal continuum.
- CDOM/*f*DOM proportions fluvial may influence the carbonate system of coastal.
- River with high CDOM proportions have implications for mussel farming.
- High CDOM/*f*DOM proportion be associated with corrosive conditions in river waters.

## GRAPHICAL ABSTRACT

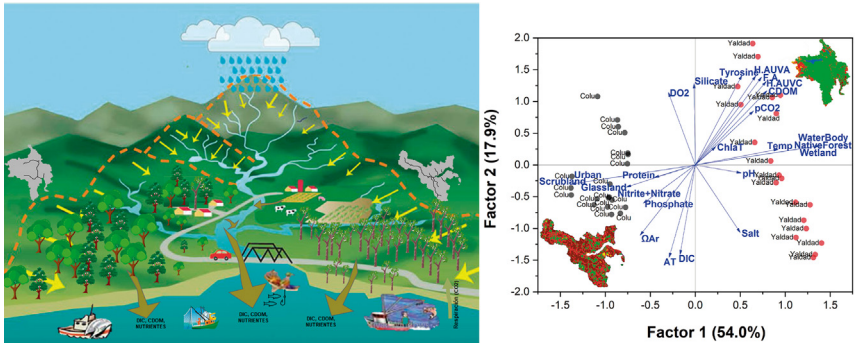


## ARTICLE INFO

*Article history:*
Received 25 June 2021
Received in revised form 14 September 2021
Accepted 15 September 2021
Available online 21 September 2021

Editor: Ashantha Goonetilleke

*Keywords:*
Land use
Colored dissolved organic matter

## ABSTRACT

Human activities have led to an increase in land use change, with effects on the structure and functioning of ecosystems. The impact of contrasting land uses along river basins on the concentration of colored dissolved organic matter (CDOM) reaching the coastal zone, and its relationship with the carbonate system of the adjacent coastal ocean, is poorly known. To understand the relationship between land use change, CDOM and its influence on the carbonate system, two watersheds with contrasting land uses in southern Chile were studied. The samples were collected at eight stations between river and adjacent coastal areas, during three sampling campaigns in the austral summer and spring. Chemical and biological samples were analyzed in the laboratory according to standard protocols. Landsat 8 satellite images of the study area were used for identification and supervised classification using remote sensing tools. The Yaldad River basin showed 82% of native forest and the Colu River basin around 38% of grassland (agriculture). Low total alkalinity ($A_T$) and Dissolved Inorganic Carbon (DIC), but high CDOM proportions were typically observed in freshwater. A higher CDOM and humic-like compounds concentration

* Corresponding author at: Facultad de Ciencias Ambientales, Universidad de Concepción, Concepción, Chile.
*E-mail address:* crvargas@udec.cl (C.A. Vargas).

https://doi.org/10.1016/j.scitotenv.2021.150435

Mussel-farming activity
Carbonate chemistry

was observed along the river-coastal ocean continuum in the Yaldad basin, characterized by a predominance of native forests. In contrast, nutrient concentrations, $A_T$ and DIC, were higher in the Colu area. Low $CaCO_3$ saturation state ($\Omega_{Ar} < 2$) and even undersaturation conditions were observed at the coastal ocean at Yaldad. A strong negative correlation between $A_T$, DIC and $\Omega_{Ar}$ with CDOM/*f*DOM, suggested the influence of terrestrial material on the seawater carbon chemistry. Our results provide robust evidence that land uses in river basins can influence CDOM/*f*DOM proportion and its influence on the carbonate chemistry of the adjacent coastal, with potential implications for the shellfish farming activity in this region.



## 1. Introduction

Land use changes have increased dramatically during the last century as a consequence of human activities, becoming one of the most critical global environmental issues worldwide (Foley et al., 2005; Barnes and Raymond, 2009; Wilson and Xenopoulos, 2009; Regnier et al., 2013; Graeber et al., 2015). Land use change (e.g., opening of areas for agriculture) causes significant alterations on the structure and functioning of aquatic ecosystems (Foley et al., 2005; Pielke, 2005; Wilson and Xenopoulos, 2009; Lambert et al., 2017), interfering with biogeochemical cycles (Stallard, 1998; Mccallister et al., 2006; Graeber et al., 2015), the provision of key ecosystem services (Conley et al., 2008; Hooper et al., 2012; Haregeweyn et al., 2015; Razali et al., 2018), among other environmental impacts. Land for agricultural use corresponds to approximately 40% of the Earth's surface cover, and affects the hydrological, biogeochemical and ecological characteristics of water bodies (Wilson and Xenopoulos, 2009; Graeber et al., 2015; Tanaka et al., 2016; Razali et al., 2018). Rivers and streams constitute one of the main carbon transport mechanisms from soils and river networks to coastal ocean (Barnes and Raymond, 2009; Bauer and Bianchi, 2011; Regnier et al., 2013).

In Chile, changing land uses through forest plantations and agro-industrial activities have expanded exponentially during the last 35 years, reducing native forest cover, from 250,000 ha in 1974 to about 3 million ha in 2016 (Salas et al., 2016; Alvarez-Garreton et al., 2019). Multiple local and regional impacts are evidenced by the land use change, chiefly in the volume and type of nutrients transported by rivers (Correa-Araneda et al., 2017; Fierro et al., 2017), and also, the ocean acidification produced by the discharge of low-alkalinity freshwater and large amounts of organic matter and nutrients to the coastal ocean (Silva et al., 2011; Vargas et al., 2013; Pérez et al., 2015; Vargas et al., 2016; Vargas et al., 2018; Lara et al., 2018; Saldías et al., 2019). For instance, Pérez et al. (2015) found that a river basin in Central Chile dominated by urban and agricultural uses showed more than twice-fold DOC concentration, and also resulted in very high DIC concentrations (>4000 μmol $kg^{-1}$).

Different studies have proven that Dissolved Organic Matter absorbance and fluorescence (CDOM/*f*DOM) measurements can be a powerful tools to characterizing its content and terrestrial inputs to seawater and to understand the relationship and implications of terrestrial material in the biogeochemistry of aquatic ecosystems (Meybeck and Vörösmarty, 2000; Coble, 2007; Wilson and Xenopoulos, 2009; Fellman et al., 2010; Petrone et al., 2011; Nelson and Siegel, 2013; Nimptsch et al., 2015; Massicotte et al., 2017; González et al., 2019; García et al., 2018, 2019). CDOM is composed of humic substances (humic acids, fulvic acids, humins), lipids, proteins and other constituents (Coble, 2007; Fellman et al., 2010; Nimptsch et al., 2015; Massicotte et al., 2017). The components of CDOM contribute to biogeochemical cycles in water and intervene in different processes such as the attenuation of sunlight in the water column, limiting primary production, and producing gases, such as $CO_2$ as a sub-product, among others (Kutser et al., 2005; Coble, 2007; García et al., 2018; Zhao et al., 2018; González et al., 2019; Sánchez-Pérez et al., 2020). On the other hand, *f*DOM sources in coastal ecosystems derive from both autochthonous material, such as phytoplankton exudates, and allochthonous subsidies from riverine discharges, such as soil detritus, and different terrestrial humic compounds (McKnight et al., 2001; Fellman et al., 2010; Nimptsch et al., 2015; Razali et al., 2018; González et al., 2019).

In consequence, changes in land use caused by human activity modify CDOM's proportion in river-coastal ocean continuum. Moreover, increasing riverine CDOM contribution to coastal ocean could fuel bacterial communities, and therefore, the $CO_2$ production (Coble, 2007; Lapierre et al., 2013; Fasching et al., 2014; Roiha et al., 2016), which in turn can alter the carbonate chemistry of the coastal ocean (e.g., pH, and carbonate availability; Schulz et al., 2009; Bauer and Bianchi, 2011; Yang et al., 2011; Bauer et al., 2013; Pérez et al., 2015; Schönberg et al., 2017; Doo et al., 2020) with potentially negative implications for marine calcifiers (Salisbury et al., 2008; Fiorini et al., 2011; Yang et al., 2011; Ashur et al., 2017; Spalding et al., 2017; Doo et al., 2019; Gao et al., 2019; Doo et al., 2020). Indeed, according to Cai (2011) estuarine waters are a significant source of $CO_2$ to the atmosphere, with a global efflux of 0.25 ± 0.25 Pg C $y^{-1}$, with partial pressure of $CO_2$ ($pCO_2$) varying from ~400–10,000 μatm. This degassing is largely supported by the respiration of terrestrial organic matter.

Different studies have focused on the origin and composition of CDOM in aquatic systems (Wilson and Xenopoulos, 2009; Fellman et al., 2010; Nimptsch et al., 2014; Nimptsch et al., 2015; Hu et al., 2017; Zhao et al., 2018; González et al., 2019) and the potential effects of changing land use on ecosystem services, such as fisheries and drinking water supply (Coble, 2007; Oyarzun et al., 2007; Hu et al., 2017; Shao and Wang, 2020). However, the connection between land use change along a river basin and the availability and concentration of the CDOM flowing into the adjacent coastal areas has been scarcely explored in the southern hemisphere (Nimptsch et al., 2014; García et al., 2018; García et al., 2019; González et al., 2019; García et al., 2020). Moreover, the influence of CDOM and *f*DOM component proportion on the carbonate system of the coastal ocean (e.g., DIC, $pCO_2$ and $A_T$), have not been studied to date.

The main objective of our study was to analyze to what extent contrasting land uses can influence the CDOM proportion found along the river-coastal ocean continuum. Additionally, we explored the potential relationship between CDOM proportion and the carbonate chemistry (DIC, total alkalinity, $pCO_2$) in the adjacent coastal zone. To this end, we use as a model system two small river basins of Chiloé Island, in northern Patagonia, Chile, with contrasting land uses (spatial scale <200 km) and an important heterogeneity in terms of geology and soil types, among others. We hypothesize that different land uses lead to variation in CDOM proportion, which, in turn, have contrasting effects on the coastal zone carbonate system. In addition, this study provides valuable information that should be taken into account in both land management strategies and marine spatial planning when considering areas for present and future human activities, such as mussel farming, of which Chile is one of the world's leading exporters (FAO, 2020).

## 2. Methods

### 2.1. Study area

The study was carried out in two river basins with contrasting land use, the Colu and Yaldad River basin, both located in Chiloé Island (42°35′39″S and 73°58′05″W), northern Patagonia, Chile (Fig. 1). The

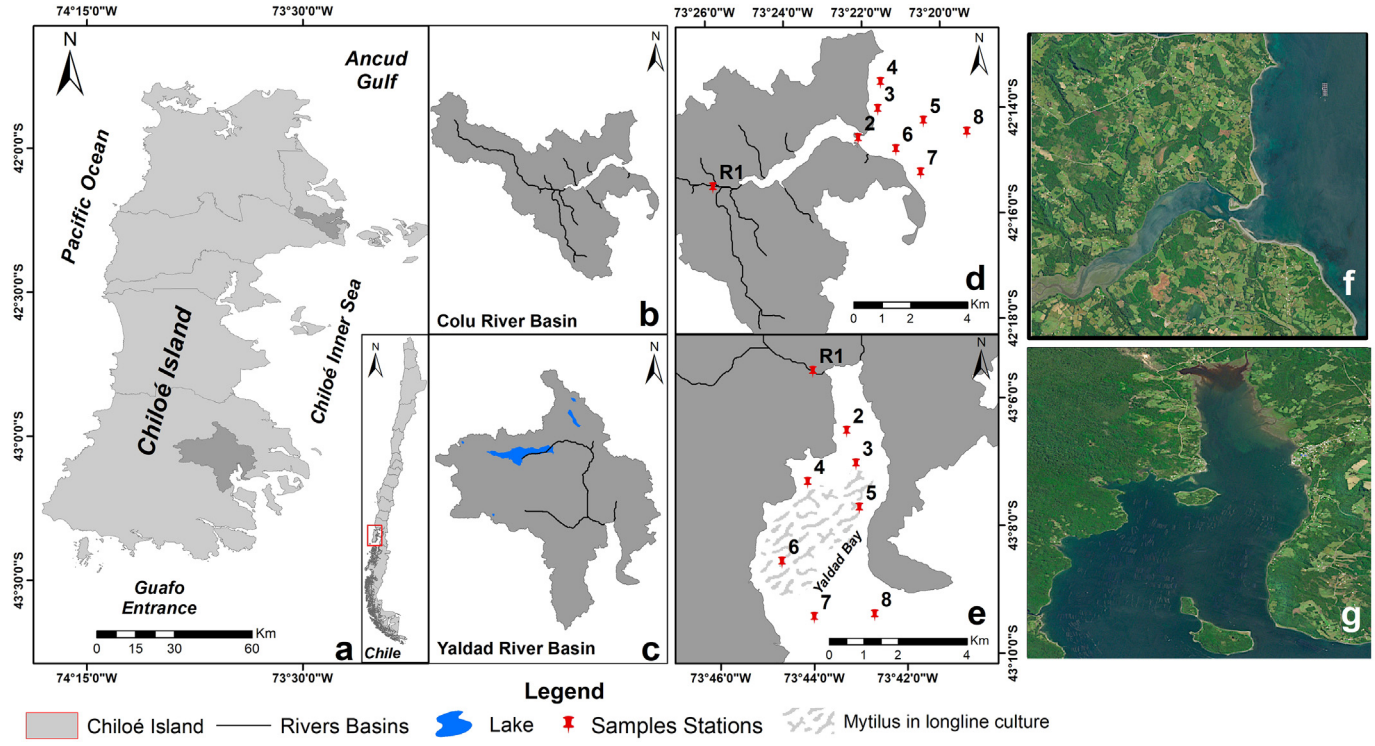


**Fig. 1.** (a) Map including a general perspective of the Chiloe Island in southern Chile, and a more detailed map highlighting the location of both river basins, (b) Colu River and the (c) Yaldad River basin. The sampling stations are also included for each river-coastal ocean continuum (d and e, respectively). The sampling stations are identified with a red pin followed by a number from 1 to 8 and the R1 initial for identified the river station. The dashed gray lines in Yaldad Bay (e) represent the location and distribution of mussel farming long-lines. High resolution (10 m) Sentinel true color composites for the regions of (f) Colu and (g) Yaldad during February 2020. (For interpretation of the references to color in this figure legend, the reader is referred to the web version of this article.)

Colu River basin (Fig. 1b) is characterized by significant land use change in contrast with the Yaldad River basin (Fig. 1c) where native forest dominates the catchment. The Colu River has an extension of 16.98 km (basin 77.31 km$^2$) and the Yaldad River has a length of 17.43 km (basin 271.06 km$^2$). Around 23% of the river basin area and the Yaldad Lake, the headwater of the river, are within a private conservation area, the Tantauco Park (Biblioteca del Congreso Nacional de Chile, www.bcn.cl and Dirección General de Agua, www.dga.cl). Both rivers originate from lagoons, lake Popetán and lake Yaldad, respectively, and discharge into the northern Patagonia Sea, one of the main mussel farming in Chile (Lagos et al., 2012; SERNAPESCA, 2018; Yévenes et al., 2021).

The local climate is temperate maritime, with an annual average temperature of 11 °C and abundant year-round rainfall, ranging from 2000 to 3000 mm year$^{-1}$, with higher intensity during the Austral winter (Subiabre and Rojas, 1994, Villalobos et al., 2003; Garreaud, 2018; Lara et al., 2018). The high rainfall feeds the rivers and lakes of the area and maintains a dense rainforest classified as Valdivian Perennial Forests (Villalobos et al., 2003; CONAF, 2014). In terms of the lithology of our studied river basins, the area is characterized by sedimentary rocks (blocks, silt, clay, gravel), and also metamorphic pelitic schists for the Yaldad river basin, in both cases characterized by silicate compounds (SERNAGEOMIN, 2003; Suchet et al., 2003). According to the World Reference Base (WRB) classification, the predominant soils in the Colu River basin are Andosols (Andosols Umbric Aluandic), derived from volcanic ash. These soils contain large amounts of organic matter and are rich in aluminum, iron oxides, and silicates (Gardi et al., 2014). The Andosols are associated with acidic materials and excess precipitation, thus providing low pH groundwater to the soils. In the Yaldad River basin, in addition to the Andosols, there are also Cambisols, which are moderately developed, removing carbonates or gypsum and forming clay minerals (Villalobos et al., 2003; Gardi et al., 2014).

The adjacent coastal area of northern Patagonia (around 9 and 8 km from the river mouth, for Colu and Yaldad River mouths, respectively), is characterized by a bathymetry with a maximum depth of 140 m (Colu from 20 to 140 m and Yaldad from 20 to 100 m), and a well-mixed water column (Pinilla, 2012). The tidal amplitude is approximately 5 m, with a semidiurnal regime (Clasing et al., 1994). Surface water temperature ranged from 6.0 °C in winter to 16.5 °C in summer in Yaldad Bay. Surface salinity fluctuated between 28 and 32 psu, dropping below 25 psu, after strong rainfall events (Clasing et al., 1994). The main economic activities in the area include fishing, agriculture, extraction of benthic macroalgae, and mussel and salmon farming (Clasing et al., 1994).

### 2.2. Sample collection

Surface water samples were collected during the morning and upon low tide conditions (~1 m depth) from the central channel at the lower reaches of Colu and Yaldad River (R1), together with their respective estuarine zones (river mouth) and the adjacent coastal areas (Colu coastal area and in Yaldad Bay) (Fig. 1d, e). Samples were obtained using a clean, sample-washed, plastic bucket. The samples were taken during two consecutive days, three field campaigns at eight sampling stations (one in the lower reaches, one at the river mouth, two samples along the narrow estuarine area, and four stations distributed in the adjacent coastal area), with a total of 48 samples per study area. Some laboratory analyses had replicates and pseudo-replicates (e.g., CDOM, nutrients, Chl *a*). The study considered three different field campaigns. Stations were visited during January 2019 and December 2019 (Austral summer) and on one occasion during November 2019 (Austral spring). Surface water samples were collected for different chemical analyses, including CDOM, Total Alkalinity ($A_T$), dissolved inorganic carbon (DIC), inorganic nutrients (including nitrate, $NO_3^-$, nitrite, $NO_2^-$,

phosphate $PO_4^{3-}$ and silicic acid $Si(OH)_4$), as well as, samples for estimates of bacterial abundance and chlorophyll-a (Chl *a*) concentration (Supplementary Material 1, SM1, Table S1 and Supplementary Material 2, SM2).

### 2.3. Hydrography, nutrients, and chlorophyll-a

The river basins were modeled using a Digital Elevations Model (DEM) obtained from the ALOS PALSAR images with a spatial resolution of 12.5 m (Alaska Satellite Facility, ASF, https://search.asf.alaska.edu/#/). Spatial Analyst's Hydrology tool was used to delimit the surface of the basins in both areas. This was complemented with previous information obtained from the Dirección General de Agua (www.dga.cl) from the Chilean Ministry of Public Works.

In the lower reaches and the river mouth, temperature, conductivity and $pH_{NBS}$ were measured immediately before water sampling using a multiparameter probe (Thermo Scientific Orion, Model Orion 3 Ross). Hydrographic characterization in the adjacent coastal ocean included vertical profiles (upper 5 m depth) of temperature (°C), salinity (psu), and dissolved oxygen (mL $L^{-1}$) by using a calibrated CTD (Seabird 19 plus V2 SeaCAT Profiler) (SM1 Table S1).

Samples for nutrient analyses were collected in triplicate and filtered through 0.7 μm (GF/F glass fiber filters), stored in 50 mL bottles, and frozen at −18 °C until analysis in the laboratory. $NO_3^-$, $NO_2^-$, $PO_4^{3-}$ and Si $(OH)_4$ were analyzed following the techniques by Atlas et al. (1971). Water samples for Chl *a* analyses were collected at the surface. For Chl *a* and phaeopigments, 200 mL of water were filtered through 0.7 μm GF/F glass fiber filters and immediately frozen (−20 °C) in the dark until further analysis by fluorometry, using acetone (90% vol/vol) for the pigment extraction (Turner 10 AU Fluorometer) according to standard procedures (Holm-Hansen and Riemann, 1978; JGOFS Protocols, 1994).

### 2.4. Estimation of the carbonate system parameters

pH (NBS scale) was measured both in freshwater and seawater samples using an Orion 3 Ross combined pH electrode, which was calibrated against three traceable pH buffers (pH 4.01, 7.00, and 10.01). Samples for $A_T$ were collected along the river-ocean continuum and poisoned with 60 μL saturated $HgCl_2$ solution and stored in 250 mL borosilicate BOD bottles with ground-glass stoppers lightly coated with Apiezon L® grease and kept in darkness at room temperature (Riebesell et al., 2010). $A_T$ was measured by Gran titration (Gran, 1952) using an open-cell (Dickson et al., 2007) semi-automatic titration system (AS-ALK2, Apollo SciTech). The AS-ALK2 system is equipped with a combination pH electrode (8302 BNUWP Ross Ultra pH/ATC Triode, Thermo Scientific, USA) connected to a pH Benchtop meter (Orion Star A211 pH meter, Thermo Scientific, USA). All samples were analyzed at 25 °C (±0.1 °C) with temperature regulation using a water-bath (Lab Companion CW-05G). The accuracy was controlled against a certified reference material (CRM, supplied by Andrew Dickson, Scripps Institution of Oceanography, San Diego, USA) and the $A_T$ repeatability averaged ±2–3 μmol $kg^{-1}$.

Samples for DIC were carefully collected in 50 mL syringes using a Tygon tube, poisoned with 10 μL of saturated $HgCl_2$ solution and then transferred to 40 mL borosilicate glass vials and kept in darkness at room temperature. The samples were analyzed using a DIC autoanalyzer (AS-C3, Apollo SciTech) by acid extraction, adding a solution of orthophosphoric acid ($H_3PO_4$) and sodium chloride (the concentration of each of these substances was 6% and 10%, respectively) and quantifying the $CO_2$ released using a non-dispersive infrared $CO_2$ detector (Goyet and Snover, 1993) (LI-COR®, model LI-7000). Measurements were calibrated with reference material (Dr. Andrew G. Dickson, Scripps Institution of Oceanography, San Diego, USA), and an accuracy of ±2 μmol $kg^{-1}$ was determined.

### 2.5. Estimation of other carbonate system parameters

Temperature, salinity, DIC and $A_T$ data were used to calculate the partial pressure of $CO_2$ ($pCO_2$) and the Saturation State of Calcium Carbonate, more specifically, Omega Aragonite ($\Omega_{Ar}$) in both estuarine and coastal waters. For zero salinity (freshwater), we employed our measurements of $pH_{NBS}$ and DIC for $pCO_2$ and $\Omega_{Ar}$ estimates since it is well known that the contribution of non-carbonate anions may overestimate river alkalinity estimates, which cannot directly contribute to $pCO_2$ (Hunt et al., 2011). Analyses were performed using the $CO_2$SYS software for MS Excel 2.1 (Pierrot et al., 2006). We have considered the dissociation constants of carbonic acid (K1 and K2) from Millero (1979) for river samples. For the estuarine and coastal zone, we used the constants K1, K2 from Lueker et al. (2000). KHSO4 was determined by Dickson (1990) for both freshwater and seawater samples.

### 2.6. Concentration and composition of colored dissolved organic matter (CDOM)

Samples were collected from surface waters and filtered by swinex with 0.2 μm GF/F filters, previously conditioned in the field with 100 mL of chromatographic water in triplicate and stored in 40 mL amber vials, previously pre-combusted for 7–8 h at 480 °C. Samples were stored (maximum 72 h) at a temperature of 4 °C until their analysis in the Laboratory of Bioassays and Applied Limnology, Institute of Marine and Limnological Sciences, Faculty of Sciences, Universidad Austral de Chile, Valdivia, Chile (Nimptsch et al., 2014; Nimptsch et al., 2015). Dissolved organic matter (DOM) presents a chromophoric and fluorescent fraction that are optically measurable, called Colored Dissolved Organic Matter or chromophore (CDOM) and fluorescent DOM (*f*DOM) (Coble, 2007; Loginova et al., 2016; Osburn et al., 2016; García et al., 2020; Sánchez-Pérez et al., 2020; Wünsch and Murphy, 2021). The absorbance of CDOM (Aλ) was determined by a UV-2401 UV–VIS spectrum of absorbance (Shimadzu, Duisburg, Germany) within wavelength range 190 to 800 nm. This measurement was converted to CDOM absorption ($m^{-1}$) according to the methodology proposed by the American Public Health Association (APHA, 2005), our absorbance coefficient was 440, also known as water color. The composition of *f*DOM was determined by fluorescence spectroscopy with an Agilent Cary Eclipse Fluorescence Spectrophotometer. The size of the cuvettes used for measurements were 1 cm for *f*DOM components (R.U) and 5 cm for CDOM ($m^{-1}$). Fluorescence was taken with 240 at 450 nm excitation wavelengths (5 nm steps) and emission from 300 to 600 nm (2 nm steps) with a slit width of 5 nm. The absorbance was scanned from 190 to 800 nm (Nimptsch et al., 2014; Nimptsch et al., 2015). Absorbance and fluorescence were measured at room temperature (25 °C) and expressed in Raman units (R.U) (Lawaetz and Stedmon, 2009). The composition and potential sources of the DOM, were estimated using a Parallel Factor Analysis Model (PARAFAC). The PARAFAC analysis identified five components, which were detected in our samples as components of the *f*DOM (SM1, Tables S2 and S3). Those five components were classified according to Coble et al. (1998) and Fellman et al. (2010): UVC humic-like acids (H.A UVC), UVA humic-like acids (H.A UVA), Protein-like, Fulvic-like acids (F.A) and Tyrosine-like (Coble et al., 1998; Fellman et al., 2010; Murphy et al., 2010; Cawley et al., 2012; Nimptsch et al., 2015; González et al., 2019). The five PARAFAC components identified were split-half validated (SM1, Figs. S1 and S2), and the best model fit was established by random initialization (Stedmon and Bro, 2008).

### 2.7. Bacterioplankton abundance

Samples for bacterial abundance (cells $mL^{-1}$) were preserved in sterile 50 mL vials and fixed with 2% *v*/v glutaraldehyde. For freshwater and seawater samples, 7 and 5 mL were filtered, respectively, and stained with 300 and 250 μL of 4′, 6-diamidino 2-phenylindole (DAPI),

respectively. All samples were filtered under a low-pressure vacuum (<80 mm Hg) on black polycarbonate filters (0.2 μm pore size). Bacterioplankton abundance (BA) was counted by epifluorescence microscopy (Porter and Feig, 1980) using a microscope OLYMPUS® IX-51 model U-MWU2 (with UV filter for DAPI, with 1000× magnification, plus 10× eyepieces). Bacterial biomass was estimated using a conversion factor of 20 fg C cell$^{-1}$ (Lee and Fuhrman, 1987). The abundance of organisms was expressed as the number of cells per volume cells mL$^{-1}$ (Porter and Feig, 1980).

### 2.8. Land uses classification from satellite images

The land cover of the two study areas was obtained from the Landsat 8 OLI image classification for images recorded in 2020. The images were obtained from the USGS Earth Explorer website (USGS Earth Explorer, https://earthexplorer.usgs.gov/) of data set Landsat Collection Level-1. The processing of the images includes radiometric, geometric and topographic corrections, with a spatial resolution of 30 m. Categorization was made from six easily identifiable land cover types: (1) native forest, (2) scrubland, (3) coverless, (4) grasslands (includes crop rotations, agriculture, livestock and grasslands improved with phosphorus mainly fertilizers), (5) water bodies (rivers, lakes and lagoons) and (6) wetlands. These categories were simplified and adapted from the "General System of Classification of Vegetation" developed for the project "Inventory and Evaluation of Native Plant Resources in Chile" (CONAF, 2014).

The supervised classification method was used to identify ground cover on the satellite images. This method consisted of selecting representative areas of each land use (Chuvieco, 1998; Chuvieco, 2010; Aguayo et al., 2009; Yin et al., 2017; Chen et al., 2020; Hao et al., 2021). The statistical criterion of maximum likelihood (Aguayo et al., 2009; Chuvieco, 2010) was chosen to build the spectral signature to classify the images according to the previously defined categories. This was supported by the Confusion Matrix method, which evaluates the accuracy of the classification (Chuvieco, 1998; Chuvieco, 2010), and complemented with three sources of information: the cartographic database of the Cadastre and Evaluation of Native Vegetation Resources of Chile, of the zones (CONAF, 2014), high-resolution images available in Google Earth (http://earth.google.com), and 99 control points taken in the field for those coverages that presented greater confusion (López et al., 2001; Aguayo et al., 2009; Hao et al., 2021). The software used was the open source QGIS 3.14 (OSGeo Foundation).

### 2.9. Statistical analysis

A two-way analysis of variance (two-way ANOVA) was used to compare physico-chemical parameters between campaigns (3 levels: January, November, December) and zones (2 levels: Colu and Yaldad) for the sampling stations located in the coastal zone. In the case of the single sampling stations located at the rivers, we used *t*-tests compare the physico-chemical parameters both study zones pooling samples across campaigns. Spearman rank correlations were used to examine the non-parametric relationships between nutrient concentration, CDOM and inorganic carbon system (DIC, $A_T$, $pCO_2$ and $\Omega_{Ar}$). We tested the influence of river and seawater on the CDOM, *f*DOM components with the carbonate system using linear regression. To synthesize the multivariate relationships among the physical-chemical characteristics of the seawater and land use patterns of both river basins, we carried out a principal component analysis (PCA) on the environmental data and land use data. Finally, a literature review was conducted to correlate land use with CDOM and *f*DOM components. Variables were normalized for statistical analyses by lg10 (Temp., Salt, OD, Chl *a*, nutrients, $A_T$, DIC, $pCO_2$, $\Omega_{Ar,}$ CDOM, *f*DOM components), square root (Bacterial Abundance), and square root (Bacterial Abundance). The analyses can be reviewed in Supplementary Material 3 (SM3).

## 3. Results

### 3.1. Hydrography

Considering both study areas, water surface temperature along the river-coastal ocean continuum fluctuated between 10 and 16 °C (SM1, Fig. S3a). The highest temperatures were recorded in Colu compared to the Yaldad area in January and December (Austral summer), with 16.4 and 16 °C for Colu and Yaldad, respectively. In contrast, low temperatures were observed during November (Austral spring) with lowest value of 10.7 °C for Colu (SM1, Fig. S3a). Significant differences in surface water temperature in the coastal zone where observed between areas (two-way ANOVA, Zone, df = 1, F = 193.935, $p < 0.001$), between campaigns (two-way ANOVA, Campaign, df = 2, F = 41.045, $p < 0.001$), and a significant interaction between zones and campaigns (two-way ANOVA, interaction Zone × Campaign, df = 2, F = 30.385, $p < 0.001$; SM3, Table S1.1). We observed no significant differences between Colu and Yaldad Rivers.

We did not observe significant salinity differences between the coastal zone of Colu and Yaldad, nor between sampling campaigns (SM3, Table S1.2). However, the interaction between zones and campaigns was significant (two-way ANOVA, interaction Zone × Campaign, df = 2, F = 5.354, $p = 0.007$). The lowest salinity values were recorded during the January and December campaigns (Austral summer) for Colu (29.8 psu) and Yaldad (25.9 psu), respectively, and specifically associated with the river mouth (SM1, Fig. S3b).

Surface coastal waters were similarly and relatively well-oxygenated across the study areas and field campaigns, with values that fluctuated between 4.5 mL L$^{-1}$ and 6.1 mL L$^{-1}$ (SM1, Fig. S3c). However, a significantly lower oxygen concentration (3 to 3.8 mL L$^{-1}$) was observed in January (Austral summer) at Yaldad Bay stations (Two-way ANOVA, Campaign, df = 2, F = 172.950, $p < 0.001$, interaction Zone × Campaign, df = 2, F = 46.628, $p < 0.001$; SM3, Table S1.3).

### 3.2. Nutrient concentrations and chlorophyll-a

We registered $NO_2^-$ + $NO_3^-$ concentrations for the different campaigns along the river-coastal ocean continuum in each study site that ranged from 1.1 μM to 19.8 μM (Fig. 2), with significant differences between the coastal zone of Colu and Yaldad Bay (two-way ANOVA, Zone, df = 1, F = 377.098, $p < 0.001$) and between campaigns (two way ANOVA, Campaign, df = 2, F = 120.294, $p < 0.001$). There was a significant interaction between sampling campaigns and study zones (two-way ANOVA, interaction Zone × Campaign, df = 2, F = 74.768, $p < 0.001$; SM3, Table S1.4). A large variance (mean ± SD) was observed for average nutrient concentrations, especially $NO_2^-$ + $NO_3^-$ concentrations during the November and December campaigns in the Colu area. The $NO_2^-$ + $NO_3^-$ concentrations at the rivers were commonly lower than those observed at adjacent coastal areas (Fig. 2, SM2). Indeed, the lowest $NO_2^-$ + $NO_3^-$ concentrations were observed at the river stations (R1) with a minimum value of 1.1 μM for both rivers during the January campaign (Fig. 2), although we found significant differences between the rivers (*t*-test = 2.458, df = 22, $p = 0.022$; SM3, Table S2). The highest concentrations of $NO_2^-$ + $NO_3^-$ were observed in spring at the stations furthest from the Colu River mouth (Fig. 2a).

$PO_4^{3-}$ concentrations fluctuated between 0.02 and 2.69 μM in both study areas (Fig. 2), with significant variation between zones and sampling campaigns, for marine stations (Two-way ANOVA, Zone, df = 2, F = 9.862, $p = 0.002$; Campaign, df = 2, F = 14.204, $p < 0.001$; interaction Zone × Campaign, df = 2, F = 9.321, $p < 0.001$, SM3, Table S1.5). The highest $PO_4^{3-}$ concentrations were observed in Colu bay during November and December (Fig. 2a), whereas $PO_4^{3-}$ concentration was lower in the Yaldad bay, especially during December (Fig. 2b). Significant differences were found between Colu and Yaldad rivers (*t*-test = 2.783, df = 6, $p = 0.032$; SM3, Table S2).

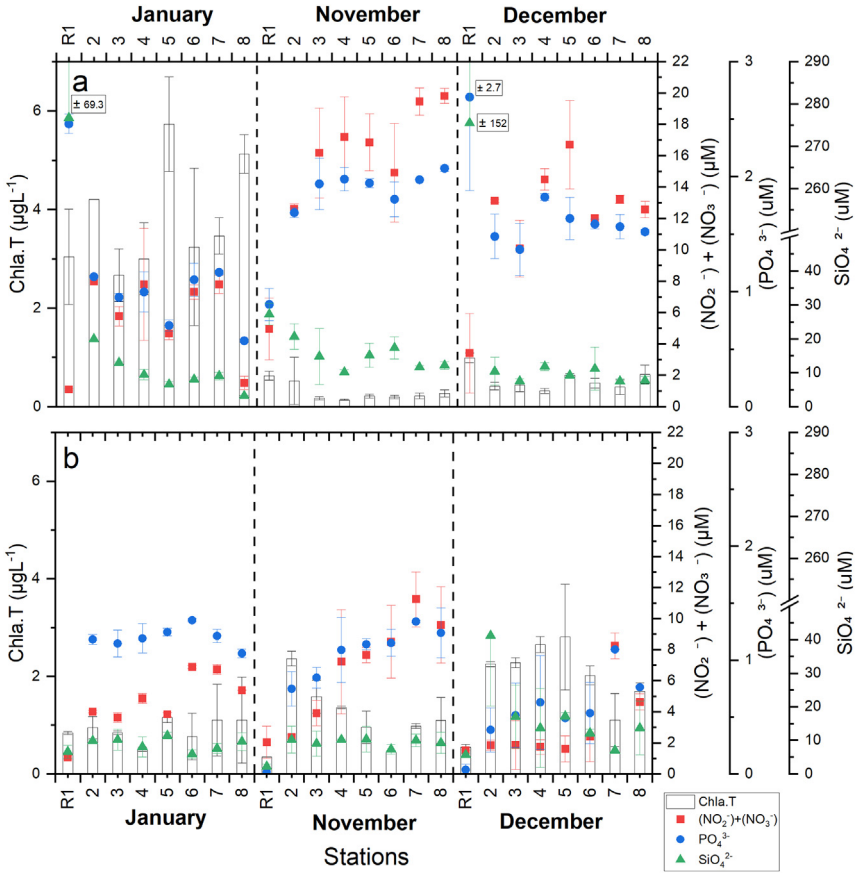


**Fig. 2.** Mean (±SD) Surface chlorophyll a and nutrient concentration ($NO_2^- + NO_3^-$, $PO_4^3$, $Si(OH)_4$) along the river-coastal ocean continuum at (a) Colu and (b) Yaldad area, during the three different campaigns (separated by vertical dashed lines). R1 represents the river station in each basin. Standard deviation values that were very large were labeled within the graph. The symbols for the variables nitrite + nitrate (red square), phosphate (blue circle) and silicate (green triangle) represent the parameter values at each sampling station. The bar above each symbol represents the standard deviation. (For interpretation of the references to color in this figure legend, the reader is referred to the web version of this article.)

Surface $Si(OH)_4$ concentration ranged from 2.17 to 276.73 µM. Significant differences were observed between campaigns in both coastal zones (Two-way ANOVA, Campaign, df = 2, F = 9.966, $p < 0.001$; interaction Zone × Campaign, df = 2, F = 21.247, $p < 0.001$; SM3, Table S1.6). On the contrary, differences were not significant between the Colu coastal ocean and Yaldad Bay. Indeed, concentrations in the Colu River basin, $Si(OH)_4$ were typically higher at the river mouth (R1) and estuarine area (Stn 2), than adjacent coastal areas (Fig. 2a). In contrast, the lowest $Si(OH)_4$ concentration between rivers, was observed at Yaldad River (R1) (Fig. 2b; *t*-test = 3.933, df = 21, $p = 0.001$).

Surface Chl *a* concentration was highly variable along the river-coastal ocean continuum, both spatially and temporally (Fig. 2). A large variance (mean ± SD) was observed among Chl *a* concentrations, especially during January and December campaigns in Colu and Yaldad coastal areas, respectively. Surface Chl *a* concentration showed significant differences only between campaigns in Colu coastal zone and Yaldad Bay (Two-way ANOVA, Campaign, df = 2, F = 133.827, $p < 0.001$; interaction Zone × Campaign, df = 2, F = 290.406, $p = 0.002$; SM3, Table S1.7). The highest Chl *a* concentrations in the adjacent coastal area were observed in Austral summer for Colu River basin (5.73 µg $L^{-1}$, January), and Yaldad River basin (2.81 µg $L^{-1}$, December). Significant differences were found between Colu and Yaldad rivers (*t*-test = 3.346, df = 34, $p = 0.001$). Indeed, low Chl *a* concentrations were typically associated to high nutrient loads in both coastal areas (Fig. 3. Spearman $R^2 = -0.62$, $p < 0.001$ for $NO_2^- + NO_3^-$ and Spearman $R^2 = -0.59$, $p \leq 0.001$ for $PO_4^{3-}$). This significant correlation between Chl and nutrients ($NO_2^- + NO_3^-$, $PO_4^{3-}$, Fig. 3) was most marked at the Colu River area (Fig. 2a).

### 3.3. Carbonate system along the river-coastal ocean continuum

The $pH_{NBS}$ along the river-coastal ocean continuum for both areas ranged from 6.372 to 8.324 (Fig. 4). In both areas, $pH_{NBS}$ was lower (from 6.372 to 7.643) at the river station in comparison with the estuary and adjacent coastal area (from 7.546 to 8.324), for Colu and Yaldad, respectively (Fig. 4, SM2). $pH_{NBS}$ at the river station (R1) was lower at Yaldad than Colu, with significant differences between both river stations (*t*-test = 2.628, df = 10, $p = 0.025$; SM3, Table S2). There were significant differences in coastal $pH_{NBS}$ between zones and sampling campaigns (Two-way ANOVA, Zone, df = 7, F = 123.532, $p < 0.001$; Campaign, df = 2, F = 75.185, $p < 0.001$; interaction Zone × Campaign, df = 2, F = 168.842, $p < 0.001$; SM3, Table S1.8). The lowest $pH_{NBS}$ values at the coastal stations were observed during the November campaign ($pH_{NBS}$ 7.546) in the Colu (Fig. 4a). $pH_{NBS}$ showed a strong and significant positive correlation with chlorophyll (Spearman $R^2 = 0.70$, $p < 0.001$; Fig. 3).

Along the river-coastal ocean continuum of both areas, $A_T$ and DIC ranged widely from 28.6 to 2203.4 and 22.5 to 2181.7 µmol $kg^{-1}$, respectively (Fig. 4, SM2), mostly due to very low $A_T$ and DIC values observed in the river station (R1) of both areas. A large standard deviation (mean ± SD) was observed for the average $A_T$ and DIC concentrations, especially during the December campaigns in the Yaldad area (Fig. 4b). Riverine DIC concentration was significantly different between river basins, with significantly higher DIC values observed at Colu River (273 to 746 µmol $kg^{-1}$), than Yaldad River (19.2 to 52.2 µmol $kg^{-1}$) (*t*-test = 3.450, df = 7, $p = 0.011$, SM3, Table S2). Something similar happened with $A_T$, where the lowest values between rivers were recorded during the December campaign in the Yaldad River

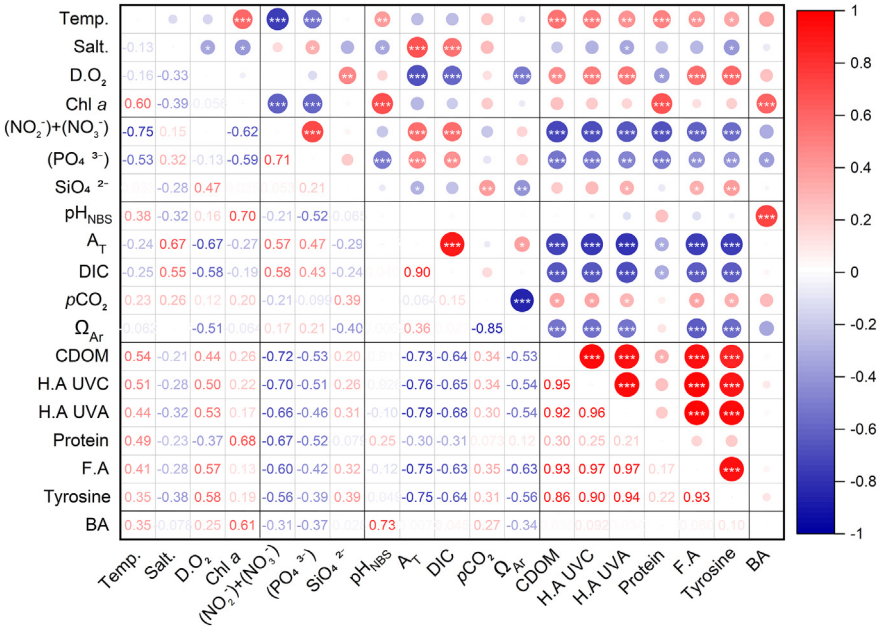


**Fig. 3.** Spearman correlation rank for all the physical-chemical variables determined along the river-coastal ocean continuum at both river basins. The color represents whether the correlation is positive (red) or negative (blue), whereas the color and the size of the circle represents the intensity of the correlation. The larger the circle, the stronger the correlation. The asterisks inside each circle (*) indicate the correlation significance (*$p \leq 0.05$, **$p \leq 0.01$ and ***$p \leq 0.001$). (For interpretation of the references to color in this figure legend, the reader is referred to the web version of this article.)

(28.6 μmol $kg^{-1}$) (t-test = 3.393, df = 9, $p = 0.008$; SM3, Table S2). Significant differences were observed between zones and sampling campaigns in Colu coastal zone and Yaldad Bay for $A_T$ (Two-way ANOVA, Zone, df = 1, F = 21.465, $p < 0.001$ and Campaign, df = 2, F = 13.321, $p < 0.001$; interaction Zone × Campaign, df = 2, F = 15.904, $p < 0.001$; SM3, Table S1.9) and DIC (Two-way ANOVA, Zone, df = 1, F = 8.550, $p = 0.005$ and Campaign, df = 2, F = 8.448, $p < 0.001$; interaction Zone × Campaign, df = 2, F = 6.037, $p = 0.004$; SM3, Table S1.10), respectively. $A_T$ and DIC showed a strong and significant positive correlation (Fig. 3, Spearman $R^2 = 0.90$, $p < 0.001$).

Similar to other carbonate system parameters, $pCO_2$ was extremely heterogeneous along the river-coastal ocean continuum, ranging from 186.4 μatm to 1849.5 μatm (Fig. 5). High $pCO_2$ (1720 μatm) was observed at Colu River during both January and November (Fig. 5a, R1). In contrast, despite the low $pH_{NBS}$ observed at Yaldad River (6.37 to 6.65), the low DIC concentration (<50 μmol $kg^{-1}$) determined a relatively low $pCO_2$ (<500 μatm) during all sampling periods (SM2). A large variance (mean ± SD) was observed for the average $pCO_2$ concentrations, especially during the December campaigns in the Yaldad area (Fig. 5b). $pCO_2$ levels were significantly different between both river (*t*-test = 4.007, df = 7, $p = 0.005$, SM3, Table S2), with lower $pCO_2$ at Yaldad area (mostly <200 μatm) in comparison to Colu area (from 500 to 1717 μatm). Similarly, significant differences between zones and sampling campaigns were observed in the $pCO_2$ of the coastal zone of Colu and Yaldad Bay (Two-way ANOVA, Zone, df = 1, F = 7.985, $p = 0.006$; Campaign, df = 2, F = 5.089, $p = 0.008$; interaction Zone × Campaign, df = 2, F = 8.384, $p = 0.001$; SM3, Table S1.11).

$\Omega_{Ar}$ during the study ranged from 0.47 to 2.83 (Fig. 5). A large standard deviation (mean ± SD) was observed for the average $\Omega_{Ar}$

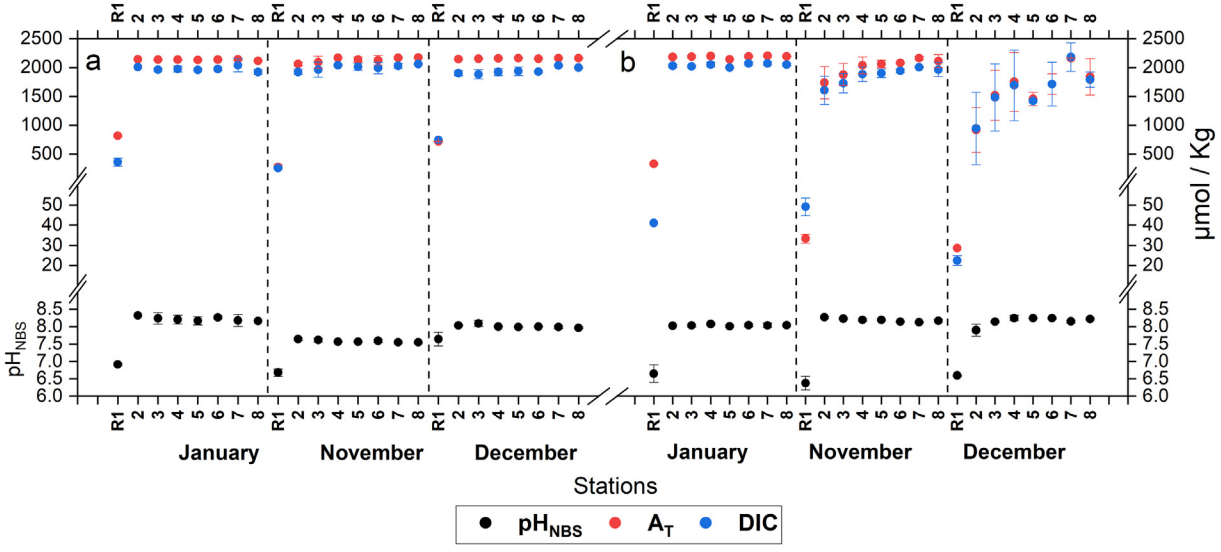


**Fig. 4.** Mean (±SD) surface $pH_{NBS}$, total alkalinity ($A_T$), and dissolved inorganic carbon (DIC) along the river-coastal ocean continuum at (a) Colu and (b) Yaldad area, during the three different campaigns (separated by vertical dashed lines). R1 represents the river station in each basin.

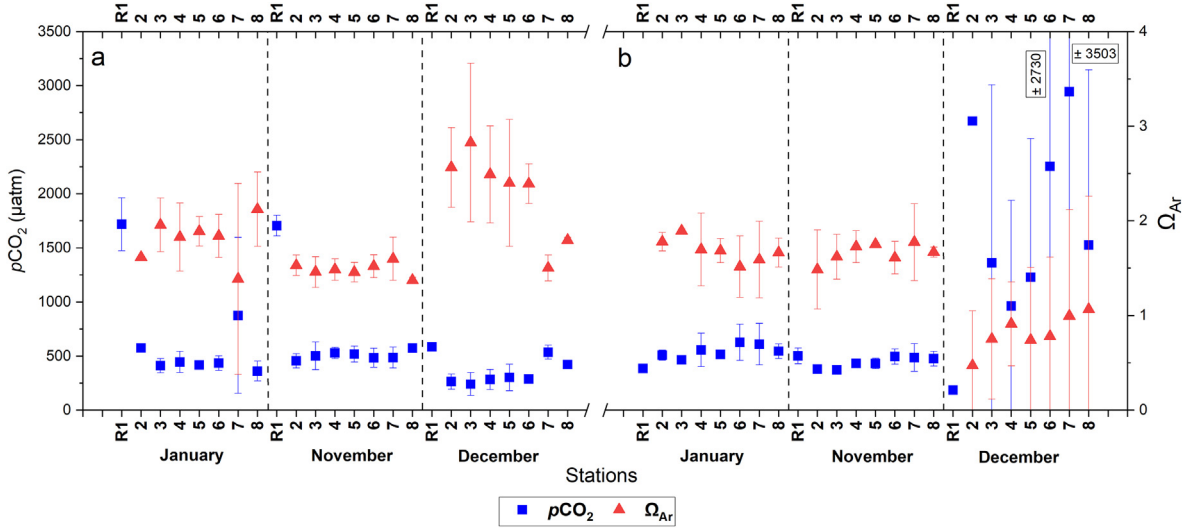


**Fig. 5.** Mean (±SD) surface partial pressure values of $CO_2$ ($pCO_2$) and saturation state of aragonite ($\Omega_{Ar}$) along the river-coastal ocean continuum at (a) Colu and (b) Yaldad area, during the three different campaigns (separated by vertical dashed lines). R1 represents the river station in each basin. Standard deviation values that were very large were labeled within the graph.

concentrations, especially during the December campaigns in the Yaldad area (Fig. 5b). Significant differences were observed between Colu coastal zone and Yaldad Bay (Two-way ANOVA, Zone, df = 1, F = 27.322, $p < 0.001$; interaction Zone × Campaign, df = 2, F = 31.094, $p < 0.001$; SM3, Table S1.12), but differences between sampling campaigns were not significant. The lowest $\Omega_{Ar}$ values were observed in the coastal area of Yaldad, especially during December ($\Omega_{Ar} = 0.47$). In contrast, saturated waters were observed during all sampling campaigns at the Colu river-influenced coastal area (Fig. 5a, $\Omega_{Ar}$ 1.37 to 2.83). A strong and negative significant correlation was observed between $pCO_2$ and $\Omega_{Ar}$ (Fig. 3, Spearman $R^2 = 0.85$, $p \leq 0.001$).

### 3.4. CDOM and fDOM concentration and composition

The values of CDOM and the *f*DOM components (UVC humic-like acids, UVA humic-like acids and Fulvic-like acids, Fig. 6) were significantly different (*t*-test, $p \leq 0.05$) between Colu and Yaldad River (SM3, Table S2). There were no significant differences between rivers for Protein-like and Tyrosine-like components (SM3, Table S2). Particularly, CDOM was significantly higher both in the river and adjacent coastal ocean at Yaldad area than Colu. Maximum CDOM proportions at the river station were different between Colu and Yaldad (R1, 2.77 and 5.34 $m^{-1}$, respectively; *t*-test = −9.574, df = 10, $p < 0.001$). Significant differences were observed for CDOM and all *f*DOM parameters, between zones and sampling campaigns, in the Colu coastal ocean and Yaldad Bay (Two-way ANOVA, Zone, Campaign, interaction Zone × Campaign, $p < 0.006$, SM3, Tables S1.13, S1.14, S1.15, S1.16, S1.17 and S1.18). Humic acids, especially Humic-like acids UVC were significantly higher (Two-way ANOVA, Zone, df = 1, F = 100.531, $p < 0.001$; campaign, df = 2, F = 30.492, $p < 0.001$; interaction Zone × Campaign, df = 2, F = 35.183, $p < 0.001$) in Yaldad Bay than Colu coastal zone (Fig. 6b and c, SM3, Table S1.14). Protein-like components were higher during January in the adjacent coastal ocean at the Colu area (Two-way ANOVA, Zone, df = 1, F = 7.563, $p = 0.006$; Campaign, df = 2, F = 38.104, $p < 0.001$; interaction Zone × Campaign, df = 2, F = 20.992, $p < 0.001$, Fig. 6e, SM3, Table S1.16), together with maximumal Chl *a* concentrations (Fig. 2a). There was also a strong and significant positive correlation between Chl *a* and proteins (Fig. 3, Spearman $R^2 = 0.68$, $p < 0.001$). A small standard deviation (mean ± SD) was observed for the average concentrations of CDOM and *f*DOM components during the sampling campaigns for both study areas (Fig. 6).

The Spearman correlation analyses showed a strong significant correlations ($p < 0.001$) between CDOM and components such as humic-like acids (UVC and UVA), Fulvic-like acids and Tyrosine-like (Fig. 3). Furthermore, the correlation analyses also evidenced strong negative correlation between CDOM with $A_T$ and DIC along the entire river-coastal ocean continuum (Fig. 3).

A positive linear relationship was found among CDOM, Humic-like acids (UVC, UVA), Fulvic-like acids with salinity ($R^2 = 0.5$) in both study areas (SM3, Table S3), showing an increasing contribution of humic-like DOM derived from the catchments towards the coastal river-ocean continuum. In addition, a high linear correlation ($R^2 = 0.7$) was also found among CDOM, Humic-like acids (UVC, UVA), Fulvic-like acids, salinity with DIC and $A_T$, respectively, in both study areas, (SM3, Figs. S1 and S2).

### 3.5. Bacterioplankton abundance

Bacterioplankton abundance (BA) was only analyzed in two seasons, November (Austral spring) and December (Austral summer), pooling all stations in each area (SM1, Fig. S4), BA ranged from 169 × $10^3$ to 1297 × $10^3$ cells $mL^{-1}$ (SM2). Significant differences were not found between the two rivers (*t*-test = 3.214, df = 2, $p = 0.085$). The maximum BA for the river stations was observed at Colu (300 × $10^3$ cell $mL^{-1}$) whereas the highest BA for the coastal area stations was observed at Yaldad Bay (1297 × $10^3$ cell $mL^{-1}$) in both cases during the December campaign. Significant differences were observed between zone and sampling campaign in the coastal zone of Colu and Yaldad Bay (Two-way ANOVA, Zone, df = 1, F = 22.884, $p < 0.001$ and Campaign, df = 7, F = 4.865, $p = 0.037$, SM3, Table S1.19). The Spearman correlation analyses showed a strong and significant positive correlation ($p < 0.001$) among bacterioplankton abundance with chlorophyll (Spearman $R^2 = 0.61$) and $pH_{NBS}$ (Spearman $R^2 = 0.73$). No significant correlations where observed between BA and $pCO_2$, omega nor DIC.

### 3.6. Land use

There were striking differences in land use between Colu and Yaldad basins (SM1, Fig. S5). The Colu basin exhibited reduced forest cover (~25%), scrublands and grasslands with 38% and 34% cover dominate land use, respectively (SM1, Fig. S5a). In stark contrast, the Yaldad basin showed a near-continuous cover of native forest, which covered 82% of the total area (SM1, Table S4 and Fig. S5b). The use of grasslands included agriculture, livestock grazing and grasslands improved with fertilizers (Odepa, 2009, https://www.odepa.gob.cl/).

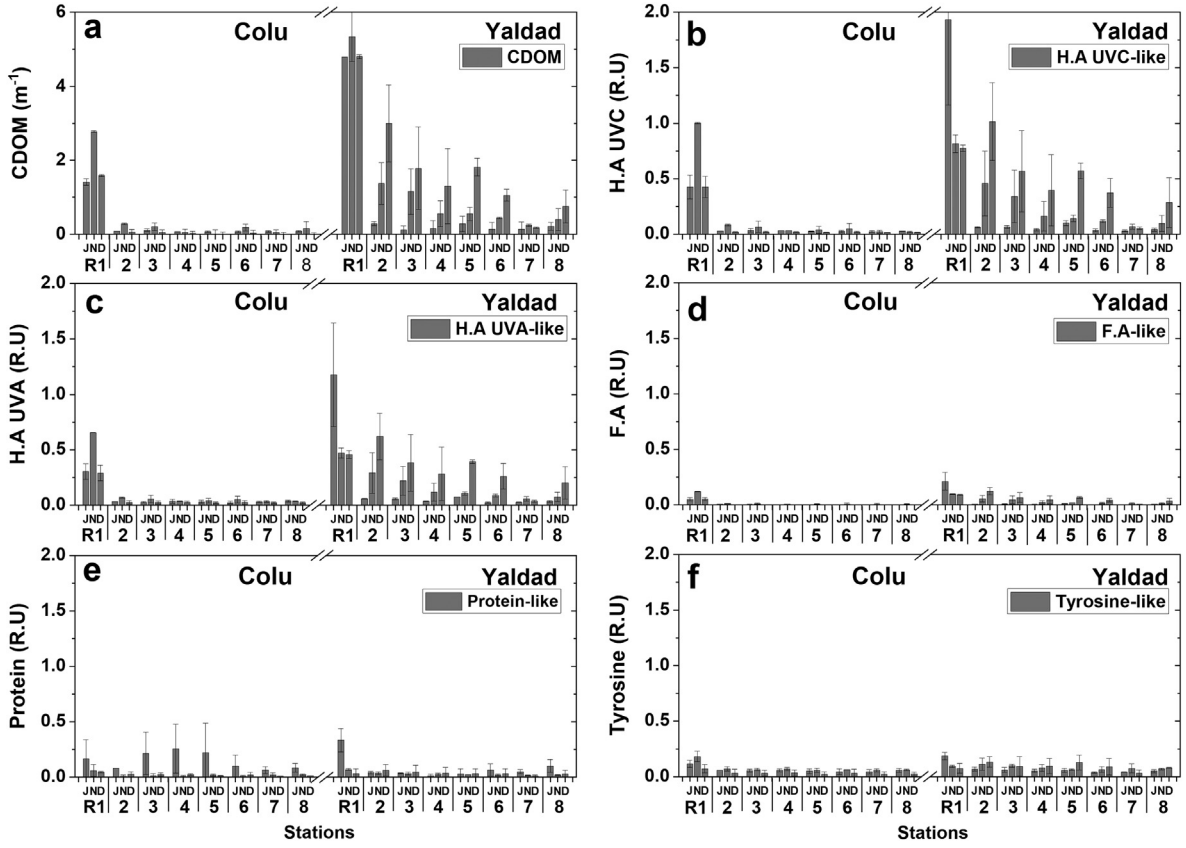


**Fig. 6.** Mean surface proportion of CDOM (a) and *f*DOM composition, including Humic-like acids UVC (H.A UVC) (b), Humic-like acids UVA (H.A UVA) (c), Fulvic-like acids (F.A) (d), Proteins-like (e) and Tyrosine-like (f), along the river-coastal ocean continuum at Colu and Yaldad area, during three different campaigns (J = January; N = November and D = December). The bar above each symbol represents the standard deviation (±SD). R1 represents the river station in each basin.

A principal component analysis (PCA) for all the stations with marine influence allowed us to examine the influence of land use as a driver of the spatial structure of the different physical/chemical parameters. The PCA performed on our environmental data yielded three principal components that together explained 84% of the total variance and the reduced dimensionality allowed for a clear separation between the two basins (Fig. 7). The first principal component (PC1) explained 54% of the interaction between variables; it was characterized by significant positive coefficients (weights > 0.6) assigned to the variables CDOM, humic-like acids (UVC and UVA), fulvic acids, tyrosine, temperature, $pCO_2$ and the land uses native forest, wetland and water body. A negative but significant coefficient was associated with nutrient concentration (nitrite + nitrate and phosphate), $A_T$, DIC, $\Omega_{Ar}$, grassland, scrubland and urban land use. Principal component two (PC2) accounted for 17% of the interaction, with a high but positive coefficient for silicate concentration, oxygen and negative for $pH_{NBS}$ and salinity. Principal component three (PC3), which explained 12%, grouped the variables protein and chlorophyll with a high and positive coefficient (Fig. 7). A grouping of the variables into four groups was observed according to the correlation and influence between them.

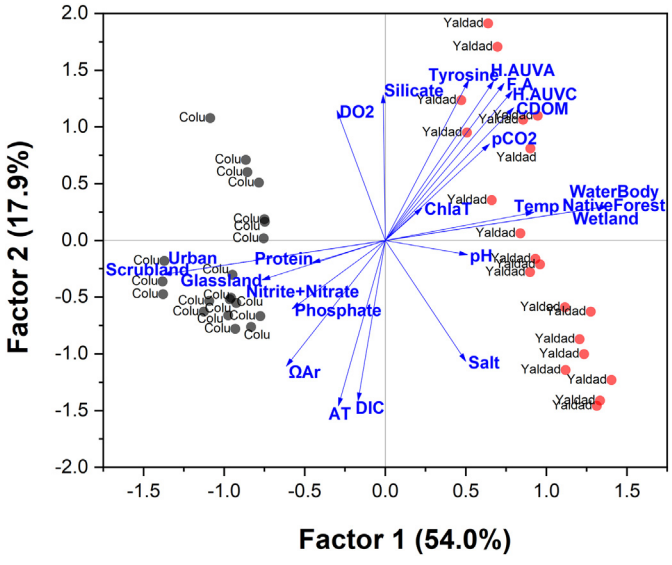


**Fig. 7.** PCA Mar Colu Yaldad. PCA-based clustering of temperature (Temp.), salinity (Salt.), dissolved oxygen ($DO_2$), chlorophyll (Chl *a*), nutrients (nitrite + nitrate, phosphorus, silicate), carbonate system ($pH_{NBS}$, $A_T$, DIC, $\Omega_{Ar}$, $pCO_2$), CDOM and humic-like acid components (H. A UVC and H.A UVA), fulvic-like acids (F.A), Protein-like, Tyrosine-like and soil uses (Glassland, Urban, Scrubland, Wetland, Native Forest, Water body). Only for the variables in Yaldad Bay (red circles) and the coastal area of Colu (black circles). The axes correspond to the first two principal components, which together explain 71% of the total variance. (For interpretation of the references to color in this figure legend, the reader is referred to the web version of this article.)

## 4. Discussion

### *4.1. Physical-chemical spatial variability along the river-ocean continuum*

In northern Patagonia, and particularly over Chiloé Island, the precipitation regime together with the lithological characteristics, and the influence of anthropogenic activities, determine the riverine contribution of nutrients and inorganic carbon to the adjacent coastal areas (Iriarte et al., 2007; Oyarzun et al., 2007; Silva, 2008; Silva and Vargas, 2014).

In our study, the highest phosphate and nitrate + nitrate concentrations were recorded in the Colu River, where land use was dominated by anthropogenic activities. Similar results from different riverine systems have shown that urban and grassland uses (agricultural and livestock) in the watersheds contribute significantly to phosphorus and nitrogen export from the river to the estuary, and then, to the adjacent coastal waters (e.g., Seitzinger et al., 2005; Stedmon et al., 2006; Barnes and Raymond, 2009; Weston et al., 2009; Savage et al., 2010; Petrone et al., 2011; Ilnicki, 2014). In contrast, in the Yaldad River, nutrient concentrations were significantly lower considering that it is a more pristine area, with a significant contribution of native forest cover (Fig. 2b). Regarding nutrient concentrations in the adjacent coastal areas influenced by these freshwater discharges, our results evidenced the influence of the contrasting land uses (SM1 Fig. S5), with higher concentrations of phosphate and nitrates at the surface of the river-coastal ocean continuum at Colu compared to Yaldad (Fig. 2a). Indeed, these results contrast previous observations in the northern Patagonia sea, where lower surface concentrations of phosphate and nitrates were found (e.g., Silva, 2008), and probably from marine origin.

Terrestrial subsidies of silica and carbon to river waters are typically influenced by the dominant weathering regimes (e.g., silicate vs. carbonate weathering; Dürr et al., 2005, 2011; Tipper et al., 2006; Zhang et al., 2009), the lithological characteristics of the basin (e.g., Amiotte et al., 2003; Dürr et al., 2005, 2011; Gurumurthy et al., 2012; Tsering et al., 2019), and precipitation (leaching from the rock) (e.g., Tipper et al., 2006; Nather-Khan and Firuza, 2010; Gurumurthy et al., 2012; Tsering et al., 2019). Nonetheless, it can be also modified by changing land uses (Amiotte et al., 2003; Conley et al., 2008; Zhang et al., 2009; Nather-Khan and Firuza, 2010; Struyf et al., 2010). Different authors have shown the importance of outcropping and weathering of silicate rocks for atmospheric $CO_2$ uptake, DIC release and alkalinity export from rivers to the adjacent sea (Amiotte et al., 2003; Tipper et al., 2006; Fortner et al., 2012). In terms of the lithology of our studied river basins, the area is characterized by silicate compounds (SERNAGEOMIN, 2003). Given the similar lithology for both basins, we would have expected that $Si(OH)_4$ concentrations were similar in both rivers. However, silica concentrations were on average higher (>150 μM) at the Colu River, which suggests that agricultural pasture use could also provide additional silica inputs to riverine waters in conjunction with other factors (e.g., pH of waters and how much mechanical or chemical erosion exists in the basin). Indeed, it has been previously reported that agricultural development (e.g., fertilizers, land clearing, deforestation) can result in increased silica input in surface runoff (stream water) and into the hydrographic basin (Barth et al., 2003; Conley et al., 2008; Zhang et al., 2009; Nather-Khan and Firuza, 2010; Fortner et al., 2012).

In terms of inorganic carbon, Barnes and Raymond (2009) conducted a similar study in small basins with different land uses, and similar hydrological characteristics than those of our study area. They observed that basins with agricultural use exported approximately 3.9 times more DIC than forested basins, as a result of accelerated chemical weathering of the rock and additions of fertilizers and manure. In our study area, DIC concentrations at the Colu River basin were on average ten times higher than in the Yaldad River basin, whose predominant land use was associated with grassland and native forest, respectively (Fig. 4, SM1 Fig. S5). In this respect, different authors have suggested that lithology and soil remobilization by anthropogenic activity such as agriculture and urbanization can release large amounts of DOM and DIC from the basin soil into the riverine water (e.g., Stedmon et al., 2006; Barnes and Raymond, 2009; Wilson and Xenopoulos, 2009; Zhang et al., 2009; Sickman et al., 2010; Petrone et al., 2011; and Graeber et al., 2015). Activities such as irrigation, land plowing, and intensive fertilization for agriculture purposes, may favor processes of rock dissolution and organic matter degradation which may contribute to increasing organic and inorganic carbon flux to the river (Barth et al., 2003; Barnes and Raymond, 2009; Abrantes et al., 2013; Graeber et al., 2015; Guo et al., 2015; Pérez et al., 2015). Based on these observations and our land use analyses, our results clearly evidence that not only high DIC concentrations but also high $pCO_2$ and $A_T$ observed at the Colu River basin could be the result of grassland – agricultural use (Figs. 4a and 5a, SM1 Fig. S5a). These results agree with observations for other small rivers and river-coastal ocean areas upon high anthropogenic disturbances (e.g., Oyarzun et al., 2007; Zhang et al., 2009; Bauer and Bianchi, 2011; Fierro et al., 2021). The physicochemical conditions in the adjacent coastal ocean showed the influence of the contrasting land use between both river basins over the seawater carbon chemistry of the adjacent coastal, where the highest DIC and $A_T$ values were observed in the river-influenced Colu coastal stations.

### 4.2. CDOM distribution along the river-ocean continuum

Patterns of land use in watersheds constitutes one of the key factors in the export of terrestrial organic matter into river systems and adjacent coastal zones (Jørgensen et al., 2011; Graeber et al., 2015; Osburn et al., 2015; Massicotte et al., 2017). This remote region of northern Patagonia contains short-length and low discharge rivers, which have been poorly studied. Unfortunately, due to the lack of information about river discharge in the area, it was not possible to quantitatively estimate the fluxes of terrigenous material into the coastal ocean. Notwithstanding, both basins share a similar topography, but the Yaldad catchment is 3.5 times larger than Colu (Fig. 1), hence larger streamflows are expected from the former than the latter. Thus, the present study is a first approximation to assess the influence of contrasting land uses on CDOM proportion and *f*DOM components in the river and adjacent coastal zone, as there is insufficient research in the river-coastal ocean continuum of northern Patagonia.

Our results show a significantly higher concentration of CDOM and *f*DOM in the adjacent coastal area of Yaldad, compared to the Colu area in northern Patagonia. These differences could be due in large part to the different land uses in these basins. It is well known that allochthonous sources of CDOM to the coastal ocean derive mainly from the degradation of terrestrial vegetation (e.g., native forests, wetlands and scrublands) and soil organic matter from tributary hydrographic basins (Coble, 2007; Nelson and Siegel, 2013; García et al., 2018; Zhao et al., 2018; Sánchez-Pérez et al., 2020). This allochthonous organic matter is constituted of a complex mixture of higher molecular weight, aromaticity and more refractory compounds, e.g., humic-like acids UVC and UVA, fulvic-like, lignin and tannins (Stedmon et al., 2007; Fellman et al., 2010; Graeber et al., 2015; Osburn et al., 2016; Roiha et al., 2016; Lambert et al., 2017; Shao and Wang, 2020).

In this sense, the Yaldad basin, with about 82% of its area covered by native forest, showed four times higher CDOM proportion than the Colu basin, which was predominantly covered by grassland and scrubland (SM1, Fig. S5). In addition, the highest concentrations of fulvic-like and humic-like acid *f*DOM components (UVC and UVA) were observed in the river stations of both basins and in the adjacent coastal area of Yaldad Bay (Fig. 6b, c and d). The autochthonous origin of CDOM and *f*DOM results from the degradation of organic matter produced in situ by living organisms (e.g., phytoplankton exudate, microbial reworking) and is mainly constituted by labile compounds (e.g., protein-like and tyrosine-like), which are rapidly mineralized by bacteria and other aquatic heterotrophs, thus releasing inorganic nutrients usable by other members of the microbial network (Williams et al., 2010; Lambert et al., 2016; González et al., 2019; Martínez-Pérez et al., 2019). Consequently, our results suggest that in our stations with a higher marine influence (Fig. 1d, e), protein-like and tyrosine-like concentrations (Fig. 6e, f) could be the result of the local autochthonous phytoplankton production, which was also evidenced by high chlorophyll concentrations (Fig. 2), especially in Yaldad Bay ($1.5 \pm 0.1$ μg $L^{-1}$). These results were similar from those observed by Nimptsch et al. (2015) and González et al. (2019) in northern Patagonia, where they reported that autochthonous tyrosine-like substances were mainly the result of bacterial metabolism and exudate from primary producers.

The PCA analysis illustrated the effects the multivariate structure highlights the role that the extensive cover of native forest and wetlands had on the concentration of CDOM and humic components in the Yaldad area and its divergence with grassland (agriculture), scrubland and urban use and nutrients (Fig. 7). At the same time, the carbonate system parameters seemed to be more strongly driven by land use in the Colu basin.

In our study, the concentration of CDOM and *f*DOM components varied in quantity along the river-coastal ocean continuum (Fig. 6), decreasing from the river to the adjacent coastal zones in both basins, as observed for different aquatic ecosystems (e.g., Wilkinson et al., 2013; Hu et al., 2017; Massicotte et al., 2017; García et al., 2018; Sánchez-Pérez et al., 2020). The spatial variation in concentrations could be associated with degradation and transformation processes undergone by CDOM and allochthonous *f*DOM components along the continuum (e.g., photobleaching, microbial consumption and production, mineralization, chemical degradation, sedimentation, flocculation and production by photosynthetic organisms) (Fasching et al., 2014; Lambert et al., 2016; Roiha et al., 2016; Massicotte et al., 2017; Martínez-Pérez et al., 2019). These processes should operate actively to decrease the molecular weight of organic matter and subsequently its reactivity along the river-coastal ocean continuum (Fasching et al., 2014; Lambert et al., 2016; Hu et al., 2017; Massicotte et al., 2017).

### 4.3. Influence or riverine CDOM and other fDOM components on the carbonate chemistry in the adjacent coastal area

The input of dissolved organic matter to aquatic ecosystem by anthropogenic processes influences $CO_2$ fluxes through processes such as eutrophication and acidification (Meybeck and Vörösmarty, 2000; Wilson and Xenopoulos, 2009; Feely et al., 2010; Regnier et al., 2013; Graeber et al., 2015). However, research focused on the influence of the allochthonous input of CDOM and *f*DOM on the carbonate system (pH, $A_T$, $pCO_2$, DIC) of the coastal zone is scarce, and difficult to assess. According to our results, the differences in land use between basins clearly influenced the CDOM and *f*DOM proportion in the rivers and the adjacent coastal zone. Moreover, the clear statistical relationships between these compounds, provides a strong indication of the influence and impacts of CDOM and *f*DOM on the surface water carbonate system parameters ($A_T$ and DIC).

Different authors argue that inputs and degradation of allochthonous organic material can change the amount and character (e.g., more or less labile) of DOM in rivers and estuaries (Stedmon and Markager, 2005; Stedmon et al., 2006; Burns et al., 2008; Bauer and Bianchi, 2011; Petrone et al., 2011). Similarly, anthropogenic inputs of organic matter also influence DIC and pH in the river-coastal ocean continuum (Barth et al., 2003; Barnes and Raymond, 2009; Feely et al., 2010). Our results showed that the Yaldad River, with predominantly native forest cover, presented the highest CDOM and *f*DOM values (SM1, Fig. 5b), while carbonate system values were the lowest ($A_T$, DIC and pH) (Fig. 4b). In contrast, the freshwater at Colu River, a grassland-dominated basin, displayed a low CDOM proportion and $pCO_2$, $A_T$, DIC values were significantly higher (Figs. 4a and 5a). These findings are in agreement with similar report suggesting that the input of allochthonous material not only increases the concentrations of dissolved and particulate organic carbon (Silva, 2008; Silva et al., 2011; McDonald et al., 2013; Cai, 2011) but also can affect other chemical parameters such as DIC, pH and $pCO_2$ (Pérez et al., 2015; McDonald et al., 2013; Cai, 2011).

In our study, statistical analyses showed that there were significant differences between zones and between sampling campaigns in river and sea stations, for parameters such as $pCO_2$, pH, DIC, $A_T$, CDOM and *f*DOM. During the December sampling campaign in the Yaldad area, it coincided with abundant rainfall and high river flow, which caused a dilution of both total alkalinity and DIC. Under low alkalinity conditions, reduced buffering capacity of river water resulted in low pH values, but not necessarily high DIC or $pCO_2$ concentration. Other authors have observed similar conditions and processes. For example Humborg et al. (2010), Cai (2011), Butman and Raymond (2011) and Lapierre et al. (2013) propose that low DIC, and consequently low $pCO_2$, conditions can occur in large rivers with high flow or in areas with high rainfall. These authors speculate on some possible causes of these conditions e.g., as river flow increased the residence time of organic matter in the water column was shorter, decreasing exposure to photochemical and bacterial decomposition. Butman and Raymond (2011) posit that regionally, carbon dioxide evasion from streams and rivers is positively correlated with annual precipitation.

CDOM was negatively correlated with $A_T$ and DIC, which could have been influenced through the co-variation with salinity, as freshwater is gradually diluted in the coastal ocean. However, the strength of the correlation was slightly higher with CDOM than with salinity (Fig. 3). CDOM was significantly higher in Yaldad, and in this area, it showed a clear trend from high CDOM/low DIC concentration in inland waters to low CDOM/high DIC in marine waters (SM3, Fig. S1c) along the salinity gradient (Fig. S2a, c). This finding could be supported by the fact that photo-production of DIC from CDOM can be an important transformation process of CDOM along the estuarine system (Guo et al., 2012). In addition, we can also observe that river-influenced waters in Yaldad were more commonly sub-saturated in terms of $CaCO_3$ ($\Omega_{Ar} < 1$), at least during our observations, in comparison to Colu (SM3, Fig. S2d).

We expected more elevated $pCO_2$ values in the river basin with higher CDOM proportions (Yaldad), but the opposite trend was observed. However, other authors (e.g., Cai, 2011; McDonald et al., 2013; Lapierre et al., 2013; Fasching et al., 2014) did not find a strong and significant correlation between $pCO_2$ and CDOM in riverine systems, as in our results (Fig. 3). These authors speculate that the CDOM proportion is one of several factors that can influence $pCO_2$ in water bodies. For example, precipitation contributes to the release of $CO_2$ to the atmosphere (Butman and Raymond, 2011) and the stream flow, turbulence and size of rivers can increase gas exchange with the atmosphere, thus lowering $pCO_2$ (Humborg et al., 2010; Lapierre et al., 2013; Cai, 2011). Moreover, the type of water (fresh or seawater) and ecosystem (river, lake, estuary, sea) also influences the interactions between chemical processes (Cai, 2011).

Nevertheless, despite we did not find a clear relationship between CDOM and $pCO_2$ at the adjacent marine area, highest $pCO_2$ levels were observed in Yaldad upon relatively high CDOM proportions. Even more, extremely high $pCO_2$ levels match with periods of high bacterioplankton abundance (SM1, Fig. S4), which could have been fueled by both autochthonous material, but with the significantly higher concentration of allochthonous organic material evidenced from the high concentration of humic-like acids in Yaldad (UVC and UVA; Fig. 6b, c). In this regard, it is known that the coastal carbonate system may be modified by photochemically and microbial processes, through degradation and respiration of both autochthonous and allochthonous CDOM, releasing $CO_2$ into seawater, which can generate an increase in $pCO_2$ (Humborg et al., 2010; Lapierre et al., 2013; Wilkinson et al., 2013; Fasching et al., 2014; Roiha et al., 2016). Moreover, the potential for biogeochemical processing, coinciding with low DIC and $A_T$ values and high CDOM and *f*DOM described above, are well aligned with the significantly lower pH observed in both rivers, particularly Yaldad (Figs. 4b and 6). On the other hand, the stable pH observed along the coastal zone stations of both study zones, was associated with low CDOM and *f*DOM values and elevated DIC and $A_T$ which significantly influence the buffer capacity of seawater. Variations in the carbonate system could be even more important during some months/periods of the year (e.g., during higher rainfall events), where an increased concentration of allochthonous terrestrial CDOM/*f*DOM could play major role on the carbonate chemistry of the adjacent coastal ocean, becoming more important than the local metabolism driven by autochthonous primary production and respiration (Feely et al., 2010; Williams et al., 2010; Bauer and Bianchi, 2011; Jørgensen et al., 2011; Lambert et al., 2016; Roiha et al., 2016; Martínez-Pérez et al., 2019).

Although the results are preliminary, they suggest that the contrasting land uses and physical-chemical degradation processes acting on the CDOM and *f*DOM components could influence the parameters of the carbonate system in the surface waters of the adjacent coastal zone. Nevertheless, our observations suggest the influence of terrestrial material (CDOM/*f*DOM) on sweater chemistry, but we still need more research effort to explore more directly the potential role of CDOM on carbonate chemistry. In consequence, we interpret our results with caution, as biogeochemical processes in the river are different from those occurring in seawater, in addition to the differences between watersheds.

### *4.4. Implications of riverine CDOM for the shellfish farming activity*

One of the main socio-economic activities of northern Patagonia is farming of *Mytilus chilensis* (*Mytilidae*, Rafinesque, 1815), an activity where Chile ranks among the top five worldwide (FAO, 2020). Most of the mussel cultivation systems in the region are located in river-influenced embayments much like the ones located near some of our sampling stations (Fig. 1e). As discussed in the previous section, native forests coverage along the Yaldad River determined a high CDOM and *f*DOM concentration along the river-coastal ocean continuum, which in turns could occasionally determine $CaCO_3$ undersaturated waters ($\Omega_{Ar} < 1$) of high $pCO_2$. Different experimental studies have demonstrated the negative impact of high $pCO_2$/low $\Omega_{Ar}$ waters on mussel's physiology (e.g., Navarro et al., 2013; Thomsen et al., 2013; Ventura et al., 2016; Saavedra et al., 2018; San Martín et al., 2019; Saavedra et al., 2020). Upon such conditions, biogenic calcification, growth, survival, immune response, and other processes can be impaired (e.g., Araneda et al., 2016; Castillo et al., 2017; Saavedra et al., 2018; Ramajo et al., 2021; Yévenes et al., 2021). Earlier studies on *M. chilensis* from Navarro et al. (2013, 2016) have reported the negative impact of high $pCO_2$ conditions on the scope of growth, one of the most sensitive measures of stress, which is also considered a suitable parameter for measuring effects on fitness (Widdows, 1985). Nevertheless, exposure to episodic events of high CDOM/*f*DOM, and high $pCO_2$ could also drive local adaptation in such mussel populations (e.g., Navarro et al., 2013; Vargas et al., 2017), and/or high food availability and/or seston concentration in this river-influenced area (as evidenced by high Chl *a* concentration, Fig. 3a) could confer them resistance to such stressful conditions. Adaptation and adaptive plasticity of organisms to environmental stressors has been studied in different aquatic ecosystems. For example, Van Colen et al. (2020) demonstrated that feeding plasticity on clam (*Scrobicularia plana*) had indirect impacts by reducing the vulnerability of herbivores to high $pCO_2$ and temperature. Ventura et al. (2016) observed that organisms such as mussel larvae (*Mytilus edulis*) have high thresholds (rate) of tolerance to acidified and sub-saturated seawater in which larval growth is sustained. Additionally, Thomsen et al. (2013) concluded that the blue mussel *Mytilus edulis* could tolerate high ambient $pCO_2$ when food supply is abundant at the Kiel Fjord (in Western Baltic Sea). Nevertheless, future research should be accomplished for exploring how persistent/chronic is this exposition to corrosive waters driven by the riverine/terrestrial CDOM export to the coastal ocean, and how marine organisms can physiologically regulate the exposition to such riverine fluxes, especially under scenarios of changing land uses, climate change, and hydrological cycles. In this context, our results are highly valuable for territorial planning strategies and marine spatial planning when considering both present and/or future areas for mussel farming activity in this and other similar coastal areas worldwide.

## 5. Summary

Our results evidence that contrasting land uses may influence the concentration of colored dissolved organic matter (CDOM/*f*DOM) in the river-coastal ocean continuum, and this in turn may influence the carbonate system ($A_T$ and DIC) of the adjacent coastal zone. Despite that the negative correlation between CDOM with $A_T$ and DIC could have been influenced through the co-variation with salinity, as freshwater is gradually diluted in the coastal ocean, the strength of the correlation was slightly higher with CDOM than with salinity. In the Yaldad basin with predominance of native forest, higher concentration of CDOM and low values of $A_T$ and DIC were observed in river and in the coastal zone. In contrast, the river basin with greater human intervention, presented significantly higher values of nutrients, $A_T$ and DIC. Overall, the results provide a first approximation demostrating that land uses along river basins can influence the concentration of CDOM/*f*DOM and on the carbonate chemistry of the adjacent coastal waters, with possible implications in the sustaintability of ecosystem services, such as shellfish farming activities.

Supplementary data to this article can be found online at https://doi.org/10.1016/j.scitotenv.2021.150435.

## CRediT authorship contribution statement

E.C-S. and C.V. conceived and designed the methodology. E.C-S. performed the sampling campaigns and data processing. M.C. and J.N. performed the analyses of the CDOM/*f*DOM and nutrient concentration laboratory samples. E.C-S., C.L., M.A. and G.S. processed and analyzed satellite images. E.C-S., C.V. and B.B. prepared the manuscript. All authors participated in the discussion, drafting and revision of the manuscript.

## Declaration of competing interest

The authors declare that they have no known competing financial interests or personal relationships that could have appeared to influence the work reported in this paper.

## Acknowledgments

This study was funded by Millennium Nucleus Center for the Study of Multiple Drivers on Marine Socio-Ecological Systems (MUSELS) funded by MINECON NC12008. The authors would like to thank L. Arias, W. García, P. Contreras, A. Cuevas, V. San Martin, D. Torres, P. Reinoso and S. Osorio for their valuable help and support during sampling and laboratory analysis. EC was funded by the National Agency for Research and Development of Chilean Government (Program BECAS-ANID) – Code 21170394. CL has been partially funded by FONDECYT 11190209 and the Millennium Nucleus Understanding Past coastal upWelling system and Environmental Local and Lasting impacts (UPWELL; NCN19_153). GS was partially supported by FONDECYT 1190805. JN acknowledges FONDECYT 1130132 & 1200205 for infrastructure used for CDOM and *f*DOM analysis. CV also thanks additional support from FONDECYT 1210171. This study was also funded by the ANID – Millennium Science Initiative Program – Code ICN2019_015.

## References

Abrantes, K.G., Barnett, A., Marwick, T.R., Bouillon, S., 2013. Importance of terrestrial subsidies for estuarine food webs in contrasting East African catchments. Ecosphere 4, 14. https://doi.org/10.1890/ES12-00322.1.

Aguayo, M., Pauchard, A., Azócar, G., Parra, O., 2009. Land use change in the south Central Chile at the end of the 20th century. understanding the spatio-temporal dynamics of the landscape. Rev. Chil. Hist. Nat. 82, 361–374. https://doi.org/10.4067/S0716-078X2009000300004.

Alaska Satellite Facility (ASF), d. ALOS PALSAR images with high spatial resolution. https://search.asf.alaska.edu/#/. (Accessed 7 May 2019).

Alvarez-Garreton, C., Lara, A., Boisier, J.P., Galleguillos, M., 2019. The impacts of native forests and Forest plantations on water supply in Chile. Forests 10, 473. https://doi.org/10.3390/f10060473.

Amiotte, S.P., Probst, J.-L., Ludwig, W., 2003. Worldwide distribution of continental rock lithology: implications for the atmospheric/soil CO2 uptake by continental weathering and alkalinity river transport to the oceans. Glob. Biogeochem. Cycles 17, 1038. https://doi.org/10.1029/2002GB001891.

APHA, 2005. Standard Methods for the Examination of Water and Wastewater. 21st edition. American Public Health Association, American Water Works Association, Water Environment Federation, Washington DC, USA.

Araneda, C., Larraín, M.A., Hecht, B., Narum, S., 2016. Adaptive genetic variation distinguishes chilean blue mussels (Mytilus chilensis) from different marine environments. Ecol. Evol. 6, 3632–3644. https://doi.org/10.1002/ece3.2110.
Ashur, M.M., Johnston, N.K., Dixson, D.L., 2017. Impacts of ocean acidification on sensory function in marine organisms. Integr. Comp. Biol. 57, 63–80. https://doi.org/10.1093/icb/icx010.
Atlas, E., Hager, S., Gordon, L., Park, P., 1971. A practical manual for use of the Technicon Autoanalyzer in sea water nutrient analyses. OSU Dept. of Oceanography, Technical Report.
Barnes, R.T., Raymond, P.A., 2009. The contribution of agricultural and urban activities to inorganic carbon fluxes within temperate watersheds. Chem. Geol. 266, 318–327. https://doi.org/10.1016/j.chemgeo.2009.06.018.
Barth, J.A., Cronin, A., Dunlop, J., Kalin, R., 2003. Influence of carbonates on the riverine carbon cycle in an anthropogenically dominated catchment basin: evidence from major elements and stable carbon isotopes in the Lagan River (N. Ireland). Chem. Geol. 200, 203–216. https://doi.org/10.1016/S0009-2541(03)00193-1.
Bauer, J.E., Bianchi, T.S., 2011. Dissolved organic carbon cycling and transformation. In: Wolanski, E., McLusky, D.S. (Eds.), Treatise on Estuarine and Coastal Science. 5. Academic Press, Waltham, Mass, pp. 7–67. https://doi.org/10.1016/B978-0-12-374711-2.00502-7.
Bauer, J.E., Cai, W.J., Raymond, P.A., Bianchi, T.S., Hopkinson, C.S., Regnier, P.A.G., 2013. The changing carbon cycle of the coastal ocean. Nature 504, 61–70. https://doi.org/10.1038/nature12857.
Biblioteca del Congreso Nacional de Chile (BCN), d. Territorial information of Chile, Mapoteca. www.bcn.cl. (Accessed 15 January 2020).
Burns, K.A., Hernes, P.J., Brinkman, D., Poulsen, A., Benner, R., 2008. Dispersion and cycling of organic matter from the Sepik River outflow to the Papua New Guinea coast as determined from biomarkers. Org. Geochem. 39, 1747–1764. https://doi.org/10.1016/J.ORGGEOCHEM.2008.08.003.
Butman, D., Raymond, P., 2011. Significant efflux of carbon dioxide from streams and rivers in the United States. Nat. Geosci. 4, 839–842. https://doi.org/10.1038/ngeo1294.
Cai, W.-J., 2011. Estuarine and coastal ocean carbon paradox: CO2 sinks or sites of terrestrial carbon incineration? Annu. Rev. Mar. Sci. 3 (1), 123–145. https://doi.org/10.1146/annurev-marine-120709-142723.
Castillo, N., Saavedra, L.M., Vargas, C.A., Gallardo-Escárate, C., Détrée, C., 2017. Ocean acidification and pathogen exposure modulate the immune response of the edible mussel Mytilus chilensis. Fish Shellfish Immunol. 70, 149–155. https://doi.org/10.1016/j.fsi.2017.08.047.
Cawley, K.M., Butler, K.D., Aiken, G.R., Larsen, L.G., Huntington, T.G., McKnight, D.M., 2012. Identifying fluorescent pulp mill effluent in the Gulf of Maine and its watershed. Mar. Pollut. Bull. 64, 1678–1687. https://doi.org/10.1016/j.marpolbul.2012.05.040.
Chen, C., He, X., Liu, Z., Sun, W., Dong, H., Chu, Y., 2020. Analysis of regional economic development based on land use and land cover change information derived from Landsat imagery. Sci. Rep. 10, 12721. https://doi.org/10.1038/s41598-020-69716-2.
Chuvieco, E., 1998. Fundamentos de teledetección espacial. Estudios Geográficos 59 135 pp.
Chuvieco, E., 2010. Teledetección ambiental: La observación de la tierra desde el espacio. Editorial Ariel Colección Ariel Ciencia Nueva. 592, p. pp.
Clasing, E., Brey, T., Stead, R., Navarro, J., Asencio, G., 1994. Population dynamics of Venus antiqua (Bivalvia: Veneracea) in the Bahía de yaldad, Isla de Chiloé, southern Chile. J. Exp. Mar. Biol. Ecol. 177, 171–186. https://doi.org/10.1016/0022-0981(94)90235-6.
Coble, P.G., 2007. Marine optical biogeochemistry: the chemistry of ocean color. Chem. Rev. 107, 402–418. https://doi.org/10.1021/cr050350.
Coble, P.G., Del Castillo, C.E., Avril, B., 1998. Distribution and optical properties of CDOM in the Arabian Sea during the 1995 southwest monsoon. Deep-Sea Res. II Top. Stud. Oceanogr. 45, 2195–2223. https://doi.org/10.1016/S0967-0645(98)00068-X.
Conley, D.J., Likens, G.E., Buso, D.C., Saccone, L., Bailey, S.W., Johnson, C.E., 2008. Deforestation causes increased dissolved silicate losses in the Hubbard brook experimental Forest. Glob. Chang. Biol. 14, 2548–2554. https://doi.org/10.1111/j.1365-2486.2008.01667.
Corporación Nacional Forestal (CONAF), 2014. Monitoreo de cambios, corrección cartográfica y actualización del catastro de recursos Vegetacionales Nativos de la Región de Los Lagos. Informe final. Universidad Austral de Chile. Región de Los Lagos, Chile. http://sit.conaf.cl.
Correa-Araneda, F., Basaguren, A., Abdala-Díaz, Roberto T., Mosele, T.A., Boyero, L., 2017. Resource- allocation tradeoffs in caddisflies facing multiple stressors. Ecol. Evol. 7, 5103–5110. https://doi.org/10.1002/ece3.309.
Dickson, A.G., 1990. Standard potential of the reaction: AgCl(s) + 1/2 H2(g) = Ag(s) + HCl(aq), and the standard acidity constant of the ion HSO4- in synthetic seawater from 273.15 to 318.15 K. J. Chem. Thermodyn. 22, 113–127.
Dickson, A.G., Sabine, C.L., Christian, J.R. (Eds.), 2007. Guide to Best Practices for Ocean CO2 Measurements, PICES. Special Publication 3. Sidney, British Columbia.
Dirección General de Agua (DGA), d. Chilean Ministry of Public Works. Hydrometeorological information. www.dga.cl. (Accessed 11 March 2020).
Doo, S.S., Edmunds, P.J., Carpenter, R.C., 2019. Ocean acidification effects on in situ coral reef metabolism. Sci. Rep. 9, 12067. https://doi.org/10.1038/s41598-019-48407-7.
Doo, S.S., Kealoha, A., Andersson, A., Cohen, A.L., Hicks, T.L., Johnson, Z.I., Long, M.H., McElhany, P., Mollica, N., Shamberger, K.E.F., Silbiger, N.J., Takeshita, Y., Busch, D.S., 2020. The challenges of detecting and attributing ocean acidification impacts on marine ecosystems. ICES J. Mar. Sci. 77, 2411–2422. https://doi.org/10.1093/icesjms/fsaa094.
Dürr, H.H., Meybeck, M., Dürr, S.H., 2005. Lithologic composition of the Earth's continental surfaces derived from a new digital map emphasizing riverine material transfer. Glob. Biogeochem. Cycles 19, GB4S10. https://doi.org/10.1029/2005GB002515.
Dürr, H.H., Meybeck, M., Hartmann, J., Laruelle, G.G., Roubeix, V., 2011. Global spatial distribution of natural riverine silica inputs to the coastal zone. Biogeosciences 8, 597–620. https://doi.org/10.5194/bg-8-597-2011.
FAO, 2020. The State of World Fisheries and Aquaculture 2020. Sustainability in Action. Rome. https://doi.org/10.4060/ca9229en.
Fasching, C., Behounek, B., Singer, G.A., Battin, T.J., 2014. Microbial degradation of terrigenous dissolved organic matter and potential consequences for carbon cycling in brown-water streams. Sci. Rep. 4, 4981. https://doi.org/10.1038/srep04981.
Feely, R.A., Alin, S.R., Newton, J., Sabine, C.L., Warner, M., Devol, A., Krembs, C., Maloy, C., 2010. The combined effects of ocean acidification, mixing, and respiration on pH and carbonate saturation in an urbanized estuary. Estuar. Coast. Shelf Sci. 88, 442–449. https://doi.org/10.1016/j.ecss.2010.05.004.
Fellman, J., Hood, E., Spencer, R.G.M., 2010. Fluorescence spectroscopy opens new windows into dissolved organic matter dynamics in freshwater ecosystems: a review. Limnol. Oceanogr. 55, 2452–2462. https://doi.org/10.4319/lo.2010.55.6.2452.
Fierro, P., Bertrán, C., Tapia, J., Hauenstein, E., Cortés, P.F., Vergara, C., Cerna, C., Vargas-Chacoff, L., 2017. Effects of local land-use on riparian vegetation, water quality, and the functional organization of macroinvertebrate assemblages. Sci. Total Environ. 609, 724–734. https://doi.org/10.1016/j.scitotenv.2017.07.197.
Fierro, P., Valdovinos, C., Lara, C., Saldías, G.S., 2021. Influence of intensive agriculture on benthic macroinvertebrate assemblages and water quality in the Aconcagua River basin (Central Chile). Water. 13, 492. https://doi.org/10.3390/w13040492.
Fiorini, S., Middelburg, J.J., Gattuso, J.-P., 2011. Effects of elevated CO2 partial pressure and temperature on the coccolithophore Syracosphaera pulchra. Aquat. Microb. Ecol. 64, 221–232. https://doi.org/10.3354/ame01520.
Foley, J.A., Defries, R., Asner, G.P., Barford, C., Bonan, G., Carpenter, S.R., Chapin, F.S., Coe, M.T., Daily, G.C., Gibbs, H.K., Helkowski, J.H., Holloway, T., Howard, E.A., Kucharik, C.J., Monfreda, C., Patz, J.A., Prentice, I.C., Ramankutty, N., Snyder, P.K., 2005. Global consequences of land use. Science 309, 570–574. https://doi.org/10.1126/science.1111772.
Fortner, S.K., Lyons, W.B., Carey, A.E., Shipitalo, M.J., Welch, S.A., Welch, K.A., 2012. Silicate weathering y CO2 consumo dentro de paisajes agrícolas, la Cuenca del río Ohio-Tennessee, EE.UU. Biogeociencias 9, 941–955. https://doi.org/10.5194/bg-9-941-2012.
Gao, K., Beardall, J., Hader, D.-P., Hall-Spencer, J.M., Gao, G., Hutchins, D.A., 2019. Effects of ocean acidification on marine photosynthetic organisms under the concurrent influences of warming, UV radiation, and deoxygenation. Front. Mar. Sci. 6, 322. https://doi.org/10.3389/fmars.2019.00322.
García, R.D., Gerea, M., García, P.E., Reissig, M., Diéguez, M.del C., 2018. Characterisation and reactivity continuum of dissolved organic matter in forested headwater catchments of Andean Patagonia. Freshw. Biol. 63, 1049–1062. https://doi.org/10.1111/fwb.13114.
García, R.D., Messetta, M.L., Feijoó, C., García, P.E., 2019. Assessment of variations in dissolved organic matter in contrasting streams in the pampas and patagonian regions (Argentina). Mar. Freshw. Res. 70, 698–707. https://doi.org/10.1071/MF18156.
García, P.E., García, R.D., Soto Cárdenas, C., Gerea, M., Reissig, M., Pérez, G.L., De Stefano, L.G., Gianello, D., Queimaliños, C., Diéguez, M.C., 2020. Fluorescence components of natural dissolved organic matter (DOM) from aquatic systems of an andean patagonian catchment: applying different data restriction criteria for PARAFAC modelling. Spectrochim. Acta A Mol. Biomol. Spectrosc. 229, 1386–1425. https://doi.org/10.1016/j.saa.2019.117957.
Gardi, C., Angelini, M., Barceló, S., Comerma, J., Cruz, G.C., Encina, R.A., Jones, A., Krasilnikov, P., Mendonça, S.B.M.L., Montanarella, L., Muñiz, U.O., Schad, P., Vara-Rodríguez, M.I., Vargas, R. (Eds.), 2014. Atlas de suelos de América Latina y el Caribe. Comisión Europea - Oficina de Publicaciones de la Unión Europea, Luxembourg.
Garreaud, R.D., 2018. Record-breaking climate anomalies lead to severe drought and environmental disruption in western Patagonia in 2016. Clim. Res. 74, 217–229. https://doi.org/10.3354/cr01505.
Gobierno de Chile, Servicio Nacional de Geología y Minería, Subdirección Nacional de Geología (SERNAGEOMIN), 2003. Mapa Geológico de Chile. Digital Geological Publication. www.ipgp.fr/~dechabal/Geol-millon.pdf.
González, H.E., Nimptsch, J., Giesecke, R., Silva, N., 2019. Organic matter distribution, composition and its possible fate in the Chilean North-Patagonian estuarine system. Sci. Total Environ. 657, 1419–1431. https://doi.org/10.1016/j.scitotenv.2018.11.445.
Goyet, C., Snover, A.K., 1993. High-accuracy mea- surements of total dissolved inorganic carbon in the ocean: comparison of alternate detection methods. Mar. Chem. 44, 235–242. https://doi.org/10.1016/0304-4203(93)90205-3.
Graeber, D., Boëchat, I.G., Encina-Montoya, F., Esse, C., Gelbrecht, J., Goyenola, G., Gücker, B., Heinz, M., Kronvang, B., Meerhoff, M., Nimptsch, J., Pusch, M.T., Silva, R.C., von Schiller, D., Zwirnmann, E., 2015. Global effects of agriculture on fluvial dissolved organic matter. Sci. Rep. 5, 16328. https://doi.org/10.1038/srep16328.
Gran, G., 1952. Determination of the equivalence point in potentiometric titrations, part II. Analyst 77, 661–671. https://doi.org/10.1039/AN9527700661.
Guo, W., Yang, L., Xiangxiang, Y., Zhai, W., Hong, H., 2012. Photo-production of dissolved inorganic carbon from dissolved organic matter in contrasting coastal waters in the southwestern Taiwan Strait, China. J. Environ. Sci. 24, 1181–1188. https://doi.org/10.1016/s1001-0742(11)60921-2.
Guo, J., Wang, F., Vogt, R.D., Zhang, Y., Liu, C.-Q., 2015. Anthropogenically enhanced chemical weathering and carbon evasion in the Yangtze Basin. Sci. Rep. 5, 11941. https://doi.org/10.1038/srep11941.
Gurumurthy, G.P., Balakrishna, K., Riotte, J., Braun, J.-J., Audry, S., Shankar, H.N.U., Manjunatha, B.R., 2012. Controls on intense silicate weathering in a tropical river, southwestern India. Chem. Geol. 300–301, 61–69. https://doi.org/10.1016/j.chemgeo.2012.01.016.
Hao, S., Zhu, F., Cui, Y., 2021. Land use and land cover change detection and spatial distribution on the Tibetan Plateau. Sci. Rep. 11, 7531. https://doi.org/10.1038/s41598-021-87215-w.
Haregeweyn, N., Tesfaye, S., Tsunekawa, A., Tsubo, M., Meshesha, D.T., Adgo, E., Elias, A., 2015. Dynamics of land use and land cover and its effects on hydrologic responses:

case study of the Gilgel Tekeze catchment in the highlands of northern Ethiopia. Environ. Monit. Assess. 187, 4090. https://doi.org/10.1007/s10661-014-4090-1.
Holm-Hansen, O., Riemann, B., 1978. Chlorophyll a determination: improvements in methodology. Oikos 30, 438–447. https://doi.org/10.2307/3543338.
Hooper, D.U., Adair, E.Carol, Cardinale, Bradley J., Byrnes, Jarrett E.K., Hungate, Bruce A., Matulich, Kristin L., Gonzalez, Andrew, Duffy, J.Emmett, Gamfeldt, Lars, O'Connor, Mary I., 2012. A global synthesis reveals biodiversity loss as a major driver of ecosystem change. Nature 486, 105–108. https://doi.org/10.1038/nature11118.
Hu, B., Wang, P., Qian, J., Wang, C., Zhang, N., Cui, X., 2017. Characteristics, sources, and photobleaching of chromophoric dissolved organic matter (CDOM) in large and shallow hongze Lake, China. J. Great Lakes Res. 43, 1165–1172. https://doi.org/10.1016/j.jglr.2017.09.004.
Humborg, C., Mörth, C.M., Sundbom, M., Borg, H., Blenckner, T., Giesler, R., Ittekkot, V., 2010. CO2 supersaturation along the aquatic conduit in swedish watersheds as constrained by terrestrial respiration, aquatic respiration and weathering. Glob. Chang. Biol. 16, 1966–1978. https://doi.org/10.1111/j.1365-2486.2009.02092.x.
Hunt, C., Salisbury, J., Vandemark, D., McGillis, W., 2011. Contrasting carbon dioxide inputs and exchange in three adjacent New England estuaries. Estuar. Coast. J ERF. 34, 68–77. https://doi.org/10.1007/s12237-010-9299-9.
Ilnicki, P., 2014. Emissions of nitrogen and phosphorus into rivers from agricultural land – selected controversial issues. J. Water Land Dev. 23, 31–39. https://doi.org/10.1515/jwld-2014-0027.
Iriarte, J.L., González, H.E., Liu, K.K., Rivas, C., Valenzuela, C., 2007. Spatial and temporal variability of chlorophyll and primary productivity in surface waters of southern Chile (41.5–43° S). Estuar. Coast. Shelf Sci. 74, 471–480. https://doi.org/10.1016/j.ecss.2007.05.015.
Joint Global Ocean Flux Study (JGOFS), 1994. Protocols. Chapter 14. Measurement of Chlorophyll a and Phaeopigments by Fluorometric Analysis . http://usjgofs.whoi.edu/JGOFS_19.pdf.
Jørgensen, L., Stedmon, C.A., Kragh, T., Markager, S., Middelboe, M., Søndergaard, M., 2011. Global trends in the fluorescence characteristics and distribution of marine dissolved organic matter. Mar. Chem. 126, 139–148. https://doi.org/10.1016/j.marchem.2011.05.002.
Kutser, T., Pierson, D.C., Kallio, K.Y., Reinart, A., Sobek, S., 2005. Mapping lake CDOM by satellite remote sensing. Remote Sens. Environ. 94, 535–540. https://doi.org/10.1016/j.rse.2004.11.009.
Lagos, L., Uriarte, I., Yany, G., 2012. Assessment of the reproductive potential of the mussel (Mytilus chilensis) from two natural populations subjected to different conditioning temperatures. Lat. Am. J. Aquat. Res. 40, 389–397. https://doi.org/10.3856/vol40-issue2-fulltext-13.
Lambert, T., Teodoru, C.R., Nyoni, F.C., Bouillon, S., Darchambeau, F., Massicotte, P., Borges, A.V., 2016. Along-stream transport and transformation of dissolved organic matter in a large tropical river. Biogeosciences 13, 2727–2741. https://doi.org/10.5194/bg-13-2727-2016.
Lambert, T., Bouillon, S., Darchambeau, F., Morana, C., Roland, F.A.E., Descy, J.-P., Borges, A.V., 2017. Effects of human land use on the terrestrial and aquatic sources of fluvial organic matter in a temperate river basin (The Meuse River, Belgium). Biogeochemistry 136, 191–211. https://doi.org/10.1007/s10533-017-0387-9.
Lapierre, J.F., Guillemette, F., Berggren, M., Del Giorgio, P.A., 2013. Increases in terrestrially derived carbon stimulate organic carbon processing and CO2 emissions in boreal aquatic ecosystems. Nat. Commun. 4, 2972. https://doi.org/10.1038/ncomms3972.
Lara, C., Saldías, G.S., Paredes, A.L., Cazelles, B., Broitman, B.R., 2018. Temporal variability of MODIS phenological indices in the temperate rainforest of northern Patagonia. Remote Sens. 10, 956. https://doi.org/10.3390/rs10060956.
Lawaetz, A., Stedmon, C., 2009. Fluorescence intensity calibration using the Raman scatter peak of water. Appl. Spectrosc. 63, 936–940. https://doi.org/10.1366/000370209788964548.
Lee, S., Fuhrman, J.A., 1987. Relationships between biovolume and biomass of naturally derived marine bacterioplankton. Appl. Environ. Microbiol. 53, 1298–1303. https://doi.org/10.1128/aem.53.6.1298-1303.1987.
Loginova, A.N., Thomsen, S., Engel, A., 2016. Chromophoric and fluorescent dissolved organic matter in and above the oxygen minimum zone off Peru. J. Geophys. Res. Oceans Res. 121, 7973–7990. https://doi.org/10.1002/2016JC011906.
López, E., Bocco, G., Mendoza, M., Duhau, E., 2001. Predicting land-cover and land-use change in the urban fringe - a case in Morelia city, México. Landsc. Urban Plan. 55, 271–285. https://doi.org/10.1016/S0169-2046(01)00160-8.
Lueker, T.J., Dickson, A.G., Keeling, C.D., 2000. Ocean pCO2 calculated from dissolved inorganic carbon, alkalinity, and equations for K1 and K2: validation based on laboratory measurements of CO2 in gas and seawater at equilibrium. Mar. Chem. 70, 105–119. https://doi.org/10.1016/S0304-4203(00)00022-0.
Martínez-Pérez, A.M., Catalá, T.S., Nieto-Cid, M., Otero, J., Álvarez, M., Emelianov, M., Reche, I., Álvarez-Salgado, X.A., Arístegui, J., 2019. Dissolved organic matter (DOM) in the open Mediterranean Sea. II: Basin–wide distribution and drivers of fluorescent DOM. Prog. Oceanogr. 170, 93–106. https://doi.org/10.1016/j.pocean.2018.10.019.
Massicotte, P., Asmala, E., Stedmon, C., Markager, S., 2017. Global distribution of dissolved organic matter along the aquatic continuum: across rivers, lakes and oceans. Sci. Total Environ. 609, 180–191. https://doi.org/10.1016/j.scitotenv.2017.07.076.
Mccallister, S., Bauer, J., Ducklow, H., Canuel, E., 2006. Sources of estuarine dissolved and particulate organic matter: a multi-tracer approach. Org. Geochem. 37, 454–468. https://doi.org/10.1016/j.orggeochem.2005.12.005.
McDonald, C.P., Stets, E.G., Striegl, R.G., Butman, D., 2013. Inorganic carbon loading as a primary driver of dissolved carbon dioxide concentrations in the lakes and reservoirs of the contiguous United States. Glob. Biogeochem. Cycles 27, 285–295. https://doi.org/10.1002/gbc.20032.
McKnight, M.D., Boyer, W.E., Westerhoff, K.P., Doran, T.P., Kulbe, T., Andersen, T.D., 2001. Spectrofluorometric characterization of dissolved organic matter for indication of precursor organic material and aromaticity. Limnol. Oceanogr. 46, 38–48. https://doi.org/10.4319/lo.2001.46.1.0038.
Meybeck, M., Vörösmarty, C., 2000. Global transfer of carbon by rivers. IGBP News Lett. 37. https://www.academia.edu/18066856/Global_transfer_of_carbon_by_rivers.
Millero, F.J., 1979. The thermodynamics of the carbonate system in seawater. Geochem. Cosmochem. Acta 43, 1651–1661. https://doi.org/10.1016/0016-7037(79)90184-4.
Murphy, K.R., Butler, K.D., Spencer, R.G.M., Stedmon, C.A., Boehme, J.R., Aiken, G.R., 2010. Measurement of dissolved organic matter fluorescence in aquatic environments: an interlaboratory comparison. Environ. Sci. Technol. 44, 9405–9412. https://doi.org/10.1021/es102362t.
Nather-Khan, I., Firuza, M., 2010. Spatial and temporal variations of silica in a disturbed Tropical River basin. Sains Malaysiana 39, 189–198.
Navarro, J.M., Torres, R., Acuña, K., Duarte, C., Manriquez, P.H., Lardies, M., Lagos, N.A., Vargas, C., Aguilera, V., 2013. Impact of medium-term exposure to elevated pCO2 levels on the physiological energetics of the mussel Mytilus chilensis. Chemosphere 90, 1242–1248. https://doi.org/10.1016/j.chemosphere.2012.09.063.
Navarro, J., Duarte, C., Manríquez, P., Lardies, M., Torres, R., Acuña, K., Vargas, C., Lagos, N., 2016. Ocean warming and elevated carbon dioxide: multiple stressor impacts on juvenile mussels from southern Chile. ICES J. Mar. Sci. J. Conseil. 73, 764–771. https://doi.org/10.1093/icesjms/fsv249.
Nelson, N.B., Siegel, D.A., 2013. The global distribution and dynamics of chromophoric dissolved organic matter. Annu. Rev. Mar. Sci. 5, 447–476. https://doi.org/10.1146/annurev-marine-120710-100751.
Nimptsch, J., Woelfl, S., Kronvang, B., Giesecke, R., González, H.E., Caputo, Jörg Gelbrecht, L., Von Tuempling, W., Graeber, D., 2014. Does filter type and pore size influence spectroscopic analysis of freshwater chromophoric DOM composition? Limnologica 48, 57–64. https://doi.org/10.1016/j.limno.2014.06.003.
Nimptsch, J., Woelfl, S., Osorio, S., Valenzuela, J., Ebersbach, P., Von Tuempling, W., Palma, R., Encina, F., Figueroa, D., Kamjunke, N., Graeber, D., 2015. Tracing dissolved organic matter (DOM) from land-based aquaculture systems in north patagonian streams. Sci. Total Environ. 537, 129–138. https://doi.org/10.1016/j.scitotenv.2015.07.160.
Odepa, 2009. La situación regional de los fertilizantes: Argentina, Brasil, Bolivia, Chile, Paraguay; Uruguay. In: Prat, Miguel Conde (Ed.), STA-CAS, IICA-CHILE. Informe, Santiago de Chile . https://www.odepa.gob.cl/.
Osburn, C.L., Mikan, M.P., Etheridge, J.R., Burchell, M.R., Birgand, F., 2015. Seasonal variation in the quality of dissolved and particulate organic matter exchanged between a salt marsh and its adjacent estuary. J. Geophys. Res. Biogeosci. 120, 1430–1449. https://doi.org/10.1002/2014JG002897.
Osburn, C.L., Boyd, T.J., Montgomery, M.T., Bianchi, T.S., Coffin, R.B., Paerl, H.W., 2016. Optical proxies for terrestrial dissolved organic matter in estuaries and coastal waters. Front. Mar. Sci. 2, 127. https://doi.org/10.3389/fmars.2015.00127.
Oyarzun, C., Aracena, C., Rutherford, P., Godoy, R., Deschrijver, A., 2007. Effects of land use conversion from native forests to exotic plantations on nitrogen and phosphorus retention in catchments of southern Chile. Water Air Soil Pollut. 179, 341–350. https://doi.org/10.1007/s11270-006-9237-4.
Pérez, C.A., DeGrandpre, M.D., Lagos, N.A., Saldías, G.S., Cascales, E.-K., Vargas, C.A., 2015. Influence of climate and land use in carbon biogeochemistry in lower reaches of rives in central southern Chile: implications for the carbonate system in river-influenced rocky shore environments. J. Geophys. Res. Biogeosci. 120, 673–692. https://doi.org/10.1002/2014JG002699.
Petrone, K.C., Fellman, J.B., Hood, E., Donn, M.J., Grierson, P.F., 2011. The origin and function of dissolved organic matter in agro-urban coastal streams. J. Geophys. Res. 116, G01028. https://doi.org/10.1029/2010JG001537.
Pielke, R.A., 2005. Land use and climate change. Science 310, 1625–1626. https://doi.org/10.1126/science.1120529.
Pierrot, D., Lewis, E., Wallace, D.W.R., 2006. MS Excel Program Developed for CO2 System Calculations. ORNL/CDIAC-105a. Carbon Dioxide Information Analysis Center, Oak Ridge National Laboratory, U.S. Department of Energy, Oak Ridge, Tennessee https://doi.org/10.3334/CDIAC/otg.CO2SYS_XLS_CDIAC105a.
Pinilla, M.E., 2012. Convenio asesoría integral Para la Toma de decisiones en Pesca y acuicultura. Determinación de las condiciones oceanográficas en las áreas Seno de Reloncaví y mar interior de Chiloé. Informe final. Instituto de Fomento Pesquero (IFOP) 147 pp.
Porter, K.G., Feig, Y.S., 1980. The use of DAPI for identifying and counting aquatic microfloral. Limnol. Oceanogr. 25, 943–948. https://doi.org/10.4319/lo.1980.25.5.0943.
Ramajo, L., Osores, S.J., Lagos, N.A., Broitman, B.R., Navarro, J.M., Vargas, C.A., Manríquez, P.H., Lardies, M.A., 2021. Estuarine condiciotns more than pH modulate the physiological flexibility of mussel perumytilus purpuratus population. Estuar. Coast. Shelf Sci. 249, 107098. https://doi.org/10.1016/j.ecss.2020.107098.
Razali, A., Syed Ismail, S.N., Awang, S., Praveena, S.M., Zainal Abidin, E., 2018. Land use change in highland area and its impact on river water quality: a review of case studies in Malaysia. Ecol. Process. 7, 19. https://doi.org/10.1186/s13717-018-0126-8.
Regnier, P., Friedlingstein, P., Ciais, P., Mackenzie, F., Gruber, N., Janssens, I., Laruelle, G., Lauerwald, R., Luyssaert, S., Andersson, A., Arndt, S., Arnosti, C., Borges, A., Dale, A., Gallego-Sala, A., Godderis, Y., Goossens, N., Hartmann, J., Heinze, C., Thullner, M., 2013. Anthropogenic perturbation of the carbon fluxes from land to ocean. Nat. Geosci. 6, 597–607. https://doi.org/10.1038/ngeo1830.
Riebesell, U., Fabry, V.J., Hansson, L., Gattuso, J.-P. (Eds.), 2010. Guide to Best Practices for Ocean Acidification Research and Data Reporting. Publications Office of the European Union, Luxembourg, p. 260.
Roiha, T., Peura, S., Cusson, M., 2016. Allochthonous carbon is a major regulator to bacterial growth and community composition in subarctic freshwaters. Sci. Rep. 6, 34456. https://doi.org/10.1038/srep34456.
Saavedra, L.M., Parra, D., San Martín, V., Lagos, N.A., Vargas, C.A., 2018. Local habitat influences on feeding and metabolic performance upon high pCO2 levels of the intertidal

mussels Perumytilius purpuratus. Estuar. Coasts 41, 1118–1129. https://doi.org/10.1007/s12237-017-0333-z.
Saavedra, L.M., Saldías, G.S., Broitman, B.R., Vargas, C.A., 2020. Carbonate chemistry dynamics in shellfish farming areas along the Chilean coast: natural ranges and biological implications. ICES J. Mar. Sci. 78, 323–339. https://doi.org/10.1093/icesjms/fsaa127.
Salas, C., Donoso, P.J., Vargas, R., Arriagada, C.A., Pedraza, R., Soto, D.P., 2016. The Forest sector in Chile: an overview and current challenges. J. For. 114, 562–571. https://doi.org/10.5849/jof.14-062.
Saldías, G., Sobarzo, M., Quinones, R., 2019. Freshwater structure and its seasonal variability off western Patagonia. Prog. Oceanogr. 174, 143–153. https://doi.org/10.1016/j.pocean.2018.10.014.
Salisbury, J., Green, M., Hunt, C., Campbell, J., 2008. Coastal acidification by Rivers: a threat to Shellfish? Eos Transactions American Geophysical Union 89, 513. https://doi.org/10.1029/2008EO500001.
San Martín, V., Gelcich, S., Vásquez-Lavin, F., Ponce, R.D., Hernández, J.I., Lagos, N.A., Birchenough, S.N.R., Vargas, C.A., 2019. Linking social preferences and ocean acidification impacts in mussel aquaculture. Nat. Sci. Rep. 9, 4719. https://doi.org/10.1038/s41598-019-41104-5.
Sánchez-Pérez, E.D., Pujo-Pay, M., Ortega-Retuerta, E., Conan, P., Marrasé, C., 2020. Mismatched dynamics of dissolved organic carbon and chromophoric dissolved organic matter in the coastal NW Mediterranean Sea. Sci. Total Environ. 746, 141190. https://doi.org/10.1016/j.scitotenv.2020.141190.
Savage, C., Leavitt, P.R., Elmgren, R., 2010. Effects of land use, urbanization, and climate variability on coastal eutrophication in the Baltic Sea. Limnol. Oceanogr. 55, 1033–1046. https://doi.org/10.4319/lo.2010.55.3.1033.
Schönberg, C.H.L., Fang, J.K.H., Carreiro-Silva, M., Tribollet, A., Wisshak, M., 2017. Bioerosion: the other ocean acidification problem. ICES J. Mar. Sci. 74, 895–925. https://doi.org/10.1093/icesjms/fsw254.
Schulz, K., Ramos, J., Zeebe, R., Riebesell, U., 2009. CO2 perturbation experiments: similarities and differences between dissolved inorganic carbon and total alkalinity manipulations. Biogeosciences 6, 2145–2153. https://doi.org/10.5194/bg-6-2145-2009.
Seitzinger, S.P., Harrison, J.A., Dumont, E., Beusen, A.H.W., Bouwman, A.F., 2005. Sources and delivery of carbon, nitrogen, and phosphorus to the coastal zone: an overview of global nutrient export from watersheds (NEWS) models and their application. Glob. Biogeochem. Cycl. 19. https://doi.org/10.1029/2005GB002606.
SERNAPESCA, Servicio Nacional de Pesca y Acuicultura. Anuario Estadístico de Pesca, 2018. Ministerio de Economía, Fomento y Turismo, Chile. Website: http://www.sernapesca.cl/.
Shao, T., Wang, T., 2020. Effects of land use on the characteristics and composition of fluvial chromophoric dissolved organic matter (CDOM) in the Yiluo River watershed, China. Ecol. Indic. 114, 106332. https://doi.org/10.1016/j.ecolind.2020.106332.
Sickman, J.O., DiGiorgio, C.L., Lee Davisson, M., Lucero, D.M., Bergamaschi, B., 2010. Identifying sources of dissolved organic carbon in agriculturally dominated rivers using radiocarbon age dating: Sacramento-San Joaquin River basin, California. Biogeochemistry 99, 79–96. https://doi.org/10.1007/s10533-009-9391-z.
Silva, N., 2008. Dissolved oxygen, pH, and nutrients in the austral Chilean channels and fjords. In: Silva, N., Palma, S. (Eds.), Progress in the Oceanographic Knowledge of Chilean Inner Waters, from Puerto Montt to Cape Horn. Comité Oceanográfico Nacional - Pontificia Universidad Católica de Valparaíso, Valparaíso, pp. 37–43.
Silva, N., Vargas, C.A., 2014. Hypoxia in chilean patagonian fjords. Prog. Oceanogr. 129, 62–74. https://doi.org/10.1016/j.pocean.2014.05.016.
Silva, N., Vargas, C.A., Prego, R., 2011. Land–ocean distribution of allochthonous organic matter in surface sediments of the Chiloé and Aysén interior seas (Chilean northern Patagonia). Cont. Shelf Res. 31, 330–339. https://doi.org/10.1016/j.csr.2010.09.009.
Spalding, C., Finnegan, S., Fischer, W.W., 2017. Energetic costs of calcification under ocean acidification. Glob. Biogeochem. Cycl. 31, 866–877. https://doi.org/10.1002/2016GB005597.
Stallard, R.F., 1998. Terrestrial sedimentation and the carbon cycle: coupling weathering and erosion to carbon burial. Glob. Biogeochem. Cycl. 12, 231–257. https://doi.org/10.1029/98GB00741.
Stedmon, C.A., Bro, R., 2008. Characterizing dissolved organic matter fluorescence with parallel factor analysis: a tutorial. Limnol. Oceanogr. Methods 6, 572–579. https://doi.org/10.4319/lom.2008.6.572.
Stedmon, C.A., Markager, S., 2005. Resolving the variability in dissolved organic matter florescence in a temperate estuary and its catchment using PARAFAC analysis. Limnol. Oceanogr. 50, 686–697. https://doi.org/10.4319/lo.2005.50.2.0686.
Stedmon, C.A., Markager, S., Søndergaard, M., Vang, T., Laubel, A., Borch, N.H., Windelin, A., 2006. Dissolved organic matter (DOM) export to a temperate estuary: seasonal variations and implications of land use. Estuar. Coasts 29, 388–400. https://doi.org/10.1007/BF02784988.
Stedmon, C.A., Thomas, D.N., Granskog, M., Kaartokallio, H., Papadimitriou, S., Kuosa, H., 2007. Characteristics of dissolved organic matter in Baltic Coastal Sea ice: allochthonous or autochthonous Origins? Environ. Sci. Technol. 41, 7273–7279. https://doi.org/10.1021/es071210f.
Struyf, E., Smis, A., Van Damme, S., Garnier, J., Govers, G., Van Wesemael, B., Conley, D.L., Batelaan, O., Frot, E., Clymans, W., Vandevenne, F., Lancelot, C., Goos, P., Meire, P., 2010. Historical land use change has lowered terrestrial silica mobilization. Nat. Commun. 1, 129. https://doi.org/10.1038/ncomms1128.
Subiabre, A., Rojas, C., 1994. Geografía Física de la Región de Los Lagos. ediciones Universidad Austral de Chile. Dirección de Investigación y desarrollo. Publicación N°4. Valdivia, p. 118.
Suchet, A.P., Probst, J.-L., Ludwig, W., 2003. Worldwide distribution of continental rock lithology: implications for the atmospheric/soil CO2 uptake by continental weathering and alkalinity river transport to the oceans. Glob. Biogeochem. Cycl. 17, 1038. https://doi.org/10.1029/2002GB001891.
Tanaka, K., Takesue, N., Nishioka, J., Kondo, Y., Ooki, A., Kuma, K., Hirawake, T., Yamashita, Y., 2016. The conservative behavior of dissolved organic carbon in surface waters of the southern Chukchi Sea, Arctic Ocean, during early summer. Sci. Rep. 6, 34123. https://doi.org/10.1038/srep34123.
Thomsen, J., Casties, I., Pansch, C., Körtzinger, A., Melzner, F., 2013. Food availability outweighs ocean acidification effects in juvenile Mytilus edulis: laboratory and field experiments. Glob. Chang. Biol. 19, 1017–1027. https://doi.org/10.1111/gcb.12109.
Tipper, E.T., Bickle, M.J., Galy, A., West, A.J., Pomiès, C., Chapman, H.J., 2006. The short term climatic sensitivity of carbonate and silicate weathering fluxes: insight from seasonal variations in river chemistry. Geochim. Cosmochim. Acta 70, 2737–2754. https://doi.org/10.1016/j.gca.2006.03.005.
Tsering, T., Abdel Wahed, M.S.M., Iftekhar, S., Sillanpää, M., 2019. Major ion chemistry of the Teesta River in Sikkim Himalaya, India: chemical weathering and assessment of water quality. J. Hydrol. Reg. Stud. 24, 100612. https://doi.org/10.1016/J.EJRH.2019.100612.
USGS Earth Explorer, d. Data Set Images of Landsat 8 Collection Level-1. https://earthexplorer.usgs.gov/. (Accessed 15 January 2020).
Van Colen, C., Ong, E.Z., Briffa, M., Wethey, D.S., Abatih, E., Moens, T., Woodin, S.A., 2020. Clam feeding plasticity reduces herbivore vulnerability to ocean warming and acidification. Nat. Clim. Chang. 10, 162–166. https://doi.org/10.1038/s41558-019-0679-2.
Vargas, C.A., Arriagada, L., Sobarzo, M., Contreras, P., Saldías, G., 2013. Bacterial production along a river-to-ocean continuum in Central Chile: implications for organic matter cycling. Aquat. Microb. Ecol. 68, 195–213. https://doi.org/10.3354/ame01608.
Vargas, C.A., Contreras, P.Y., Pérez, C.A., Sobarzo, M., Saldías, G.S., Salisbury, J., 2016. Influences of riverine and upwelling waters on the coastal carbonate system off Central Chile and their ocean acidification implications. J. Geophys. Res. Biogeosci. 121, 1468–1483. https://doi.org/10.1002/2015JG003213.
Vargas, C., Lagos, N., Lardies, M., Lardies, M.A., Duarte, C., Manríquez, P.H., Aguilera, V.M., Broitman, B., Widdicombe, S., Dupont, S., 2017. Species-specific responses to ocean acidification should account for local adaptation and adaptive plasticity. Nature Ecol. Evol. 1, 0084. https://doi.org/10.1038/s41559-017-0084.
Vargas, C.A., Cuevas, L.A., Silva, N., González, H.E., De Pol-Holz, R., Narváez, D.A., 2018. Influence of glacier melting and river discharges on the nutrient distribution and DIC recycling in the southern chilean Patagonia. J. Geophys. Res. Biogeosci. 123, 256–270. https://doi.org/10.1002/2017JG003907.
Ventura, A., Schulz, S., Dupont, S., 2016. Maintained larval growth in mussel larvae exposed to acidified under-saturated seawater. Sci. Rep. 6, 23728. https://doi.org/10.1038/srep23728.
Villalobos, L., Parra, O., Grandjean, M., Jaque, E., Woelfl, S., Campos, H., 2003. A study of the river basins and limnology of five humic lakes on Chiloé Island. Rev. Chil. Hist. Nat. 76, 563–590. https://doi.org/10.4067/S0716-078X2003000400003.
Weston, N.B., Hollibaugh, J.T., Joye, S.B., 2009. Population growth away from the coastal zone: thirty years of land use change and nutrient export in the Altamaha River, GA. Sci. Total Environ. 407, 3347–3356. https://doi.org/10.1016/j.scitotenv.2008.12.066.
Widdows, J., 1985. Physiological procedures. In: Bayne, B.L. (Ed.), The Effect of Stress and Pollution on Marine Animals. Praeger, New York, pp. 161–178.
Wilkinson, G.M., Carpenter, S.R., Cole, J.J., Pace, M.L., Yang, C., 2013. Terrestrial support of pelagic consumers: patterns and variability revealed by a multilake study. Freshw. Biol. 58, 2037–2049. https://doi.org/10.1111/fwb.12189.
Williams, C.J., Yamashita, Y., Wilson, H.F., Jaffé, R., Xenopoulos, M.A., 2010. Unraveling the role of land use and microbial activity in shaping dissolved organic matter characteristics in stream ecosystems. Limnol. Oceanogr. 55, 1159–1171. https://doi.org/10.4319/lo.2010.55.3.1159.
Wilson, H.F., Xenopoulos, M.A., 2009. Effects of agricultural land use on the composition of fluvial dissolved organic matter. Nat. Geosci. 2, 37–41. https://doi.org/10.1038/ngeo391.
Wünsch, U.J., Murphy, K., 2021. A simple method to isolate fluorescence spectra from small dissolved organic matter datasets. Water Res. 190, 116730. https://doi.org/10.1016/j.watres.2020.116730.
Yang, Y., Dai, M., Cao, Z., Huang, Z., 2011. Calcification rates of Emiliania huxleyi in different pH waters: a comparison of methods. Adv. Geosci. 24, 43–53. https://doi.org/10.1142/9789814355353_0003.
Yévenes, M., Núñez-Acuña, G., Gallardo-Escárate, C., Gajardo, G., 2021. Adaptive differences in gene expression in farm-impacted seedbeds of the native blue mussel Mytilus chilensis. Front. Genet. 12, 666539. https://doi.org/10.3389/fgene.2021.666539.
Yin, H., Khamzina, A., Pflugmacher, D., Martius, C., 2017. Forest cover mapping in post-soviet Central Asia using multi-resolution remote sensing imagery. Sci. Rep. 7, 1375. https://doi.org/10.1038/s41598-017-01582-x.
Zhang, S., Lu, X.X., Sun, H., Han, J., Higgitt, D.L., 2009. Major ion chemistry and dissolved inorganic carbon cycling in a human-disturbed mountainous river (the Luodingjiang River) of the zhujiang (Pearl River), China. China Sci. Total Environ. 407, 2796–2807. https://doi.org/10.1016/j.scitotenv.2008.12.036.
Zhao, J., Cao, W., Xu, Z., Ai, B., Yang, Y., Jin, G., Wang, G., Zhou, W., Chen, Y., Chen, H., Sun, Z., 2018. Estimating CDOM concentration in highly turbid estuarine coastal waters. J. Geophys. Res. Oceans 123, 5856–5873. https://doi.org/10.1029/2018JC013756.